

# MEDICAL JOURNAL

香港醫學雜誌

The official publication of the  
Hong Kong Academy of Medicine  
and the Hong Kong Medical Association

Research Fund for the Control of  
Infectious Diseases

Research Dissemination Reports

控制傳染病研究基金

研究成果報告

Tuberculosis

肺結核

Tuberculosis/HIV

肺結核/愛滋病病毒

HIV

愛滋病病毒

Epstein-Barr virus

人類疱疹病毒第四型



# HONG KONG MEDICAL JOURNAL

## 香港醫學雜誌

Vol 19 No 5 October 2013  
Supplement 5

Editor-in-Chief  
Ignatius TS Yu 余德新

Senior Editors  
PT Cheung 張璧濤  
CB Chow 周鎮邦  
Albert KK Chui 徐家強  
Michael G Irwin  
TW Wong 黃大偉

Editors  
KL Chan 陳廣亮  
KS Chan 陳健生  
Henry LY Chan 陳力元  
David VK Chao 周偉強  
TW Chiu 趙多和  
Stanley ST Choi 蔡兆棠  
LW Chu 朱亮榮  
WK Hung 熊維嘉  
Bonnie CH Kwan 關清霞  
Alvin KH Kwok 郭坤豪  
Paul BS Lai 賴寶山  
Eric CH Lai 賴俊雄  
Stephen TS Lam 林德深  
Patrick CP Lau 劉志斌  
Arthur CW Lau 劉俊穎  
Nelson LS Lee 李禮舜  
Danny WH Lee 李偉雄  
KY Leung 梁國賢  
Danny TN Leung 梁子昂  
Thomas WH Leung 梁慧強  
WK Leung 梁惠強  
Kenneth KW Li 李啟煌  
David TL Liu 劉大立  
Janice YC Lo 羅懿之  
Herbert HF Loong 龍浩鋒  
James KH Luk 陸嘉熙  
Ronald CW Ma 馬青雲  
Ada TW Ma 馬天慧  
Henry KF Mak 麥嘉豐  
Jacobus KF Ng 吳國夫  
Hextan YS Ngan 顏婉嫻  
Martin W Pak 白威  
Edward CS So 蘇超駒  
PC Tam 談寶維  
William YM Tang 鄧旭明  
Martin CS Wong 黃至生  
Kenneth KY Wong 黃格元  
Patrick CY Woo 胡劍逸  
Bryan PY Yan 甄秉言  
TK Yau 游子覺  
Kelvin KH Yiu 姚啟恒

Advisors on Biostatistics  
William B Goggins  
Eddy KF Lam 林國輝

Advisor on Clinical Epidemiology  
Shelly LA Tse 謝立亞

### Research Fund for the Control of Infectious Diseases

#### Research Dissemination Reports

Editorial 3

---

#### TUBERCULOSIS

---

Physiological fitness of drug-resistant *Mycobacterium tuberculosis* isolates in Hong Kong 4  
*EWC Chan, RCY Chan, MTK Au, RWM Lai*

A real-time polymerase chain reaction protocol for rapid detection of *Mycobacterium tuberculosis*, drug resistance, and Beijing genotype 8  
*ETY Leung, M Ip, EWC Chan, RCY Chan*

Genome analysis of *Mycobacterium tuberculosis* Beijing family strains 12  
*SKW Tsui, RCY Chan, KM Kam, HS Kwan, KS Leung, KP Fung, MMY Waye, PTW Law, SK Lou, KK Leung*

Effect of IL-17 on enhancing innate immunity to mycobacterial infection 15  
*WL Ling, JW Fang, VLJ Wang, ASY Lau, JCB Li*

---

#### TUBERCULOSIS/HIV

---

Suppression of cellular antibacterial effects by HIV 19  
*JCB Li, LLY Chan, HCH Yim, BKW Cheung, DCW Lee, ASY Lau*

---

#### HIV

---

Triple combination lentiviral vector-based haematopoietic stem cell gene therapy for inhibition of drug-resistant HIV-1 24  
*Y Chen, BC Wong, CH Li, X Zhang, SS Lee*

Effect of human cathelicidin and fragments on HIV-1 enzymes 27  
*JH Wong, A Legowska, K Rolka, TB Ng, M Hui, CH Cho, WW Lam, SW Au, OW Gu, DC Wan*

**International Editorial  
Advisory Board**

**Sabaratnam Arulkumaran**  
United Kingdom

**Robert Atkins**  
Australia

**Peter Cameron**  
Australia

**David Christiani**  
United States

**James Dickinson**  
Canada

**Adrian Dixon**  
United Kingdom

**Willard Fee, Jr**  
United States

**Robert Hoffman**  
United States

**Sean Hughes**  
United Kingdom

**Arthur Kleinman**  
United States

**Xiaoping Luo**  
China

**Jonathan Samet**  
United States

**Rainer Schmelzeisen**  
Germany

**Homer Yang**  
Canada

Executive Editor  
**Cyrus R Kumana**

Managing Editor  
**Yvonne Kwok 郭佩賢**

Deputy Managing Editor  
**Betty Lau 劉薇薇**

Assistant Managing Editor  
**Warren Chan 陳俊華**

---

**EPSTEIN-BARR VIRUS**

---

**Identification of Epstein-Barr virus microRNA in nasopharyngeal carcinoma cells** 31

*RWM Lung, JHM Tong, MYM Sung, SL Chau, KW Lo, KF To*

**Identification and characterisation of Epstein-Barr virus miRNA in nasopharyngeal carcinoma cells** 36

*RWM Lung, JHM Tong, MYM Sung, PPS Leung, SL Chau, DCH Ng, AWH Chan, EKO Ng, KW Lo, KF To*

**Latent-lytic switch of Epstein-Barr virus infection in gastric carcinoma** 39

*J Yu, HC Jin*

**Fine mapping candidate loci for nasopharyngeal carcinoma in southern Chinese specifically linked to Epstein-Barr virus aetiopathogenesis** 43

*Y Li, L Fu, AM Wong, YH Fan, MX Li, JX Bei, WH Jia, YX Zeng, D Chan, KM Cheung, P Sham, D Chua, XY Guan, YQ Song*

---

**Author index** 47

**Disclaimer** 48

Dissemination reports are concise informative reports of health-related research supported by funds administered by the Food and Health Bureau, namely the *Research Fund for the Control of Infectious Diseases* (RFCID) and the *Health and Health Services Research Fund* (HHSRF). In this edition, 11 dissemination reports of projects related to tuberculosis, human immunodeficiency virus (HIV), and Epstein-Barr virus are presented. In particular, three projects are highlighted due to their potentially significant findings, impact on healthcare delivery and practice, and/or contribution to health policy formulation in Hong Kong.

*Mycobacterium tuberculosis* (MTB) affects one third of the world's population and causes 1 to 2 million deaths annually. The emerging Beijing/W strain of MTB is causing worldwide alarm due to its increased transmissibility and tendency to develop multidrug resistance compared with other strains of mycobacteria. Tsui et al<sup>1</sup> conducted genome analysis of drug-resistant and drug-sensitive isolates of Beijing/W MTB from Hong Kong. The authors were able to identify novel genetic factors associated with the drug-resistance phenotype. This study had impact beyond the publication of results in peer-reviewed journals. Project team members and research staff gained additional postgraduate qualifications and career advancement after participating in this study. The study also led to additional research grants being awarded in related areas.

Coinfection of HIV-1 and MTB is important in AIDS pathogenesis. Both HIV-1 and MTB have efficient immune evasion mechanisms to subvert immunity, and both microbes and their encoded proteins act in concert to cripple cellular antimicrobial responses and enhance each other's survival and replication. Li et al<sup>2</sup> found that cytokines such as interferon-gamma may have a role in suppressing the action of HIV-1 in its enhancement of mycobacterial growth in human phagocytes. This may provide a scientific rationale for the use of interferon-gamma and related cytokines in AIDS patients with aggressive mycobacterial infections. Apart from peer-reviewed publications, this study also led to project team members and research staff gaining postgraduate qualifications, career advancement, and additional research funding.

Nasopharyngeal carcinoma (NPC) is prevalent in southern China. Epstein-Barr virus (EBV), also known as human herpesvirus 4, and EBV-encoded microRNAs (miRNAs) have been implicated in NPC carcinogenesis. Lung et al<sup>3</sup> identified two novel miRNAs and found that one of them could modulate LMP2A—an important oncogenic and immunogenic EBV gene. Knowledge of how miRNAs function in the establishment and/or maintenance of latent infections and pathogenesis in NPC cells may improve the treatment of NPC in future.

The Research Office of the Food and Health Bureau would like to take this opportunity to pay our respects to the late Prof Allan Sik-yin Lau, co-author of two reports in this supplement, who passed away earlier this year.

We hope you will enjoy this selection of research dissemination reports. Electronic copies of these dissemination reports and the corresponding full reports can be downloaded individually from the Research Fund Secretariat website (<http://www.fhb.gov.hk/grants>). Researchers interested in the funds administered by the Food and Health Bureau also may visit the website for detailed information about application procedures.

Supplement co-editors



Dr Ivy Cheung  
Chief Secretariat Executive  
(Research Office)  
Food and Health Bureau



Dr Richard A. Collins  
Scientific Review Director  
(Research Office)  
Food and Health Bureau

## References

1. Tsui SK, Chan RC, Kam KM, et al. Genome analysis of *Mycobacterium tuberculosis* Beijing family strains. *Hong Kong Med J* 2013;19(Suppl 5):12-4.
2. Li JC, Chan LL, Yim HC, Cheung BK, Lee DC, Lau AS. Suppression of cellular antibacterial effects by HIV. *Hong Kong Med J* 2013;19(Suppl 5):19-23.
3. Lung RW, Tong JH, Sung MY, et al. Identification and characterisation of Epstein-Barr virus miRNA in nasopharyngeal carcinoma cells. *Hong Kong Med J* 2013;19(Suppl 5):36-8.

EWC Chan 陳維智  
 RCY Chan 陳超揚  
 MTK Au 區大綱  
 RWM Lai 賴偉文

# Physiological fitness of drug-resistant *Mycobacterium tuberculosis* isolates in Hong Kong

## Key Messages

1. Drug target gene mutations in *Mycobacterium tuberculosis* conferred drug resistance at the expense of physiological fitness of the pathogen, rendering it less capable of multiplying even in a nutrient-rich environment.
2. Isolates containing mutations in *gyrA* experienced the strongest growth inhibition.
3. The growth fitness cost of resistance-gene mutations may only slow down mycobacterial growth at the initial phase (immediately after inoculation), possibly with little negative effect on the overall ability of this pathogen to cause disease in humans.
4. In addition to the mutation-induced effects, growth and survival fitness of multi-drug-resistant tuberculosis (MDR-TB) is also highly dependent on overall genetic constraints, which are unique to each organism.
5. Such MDR-TB mutants are fully capable of residing in human host-reservoirs and are as effective as their non-resistant counterparts in causing infections in the community.

*Hong Kong Med J* 2013;19(Suppl 5):S4-7

Department of Microbiology, The Chinese University of Hong Kong, The Prince of Wales Hospital

EWC Chan, RCY Chan, MTK Au, RWM Lai

RFICID project number: 06060132

Principal applicant and corresponding author:  
 Dr Edward Wai Chi Chan  
 Department of Microbiology, Faculty of Medicine, The Prince Wales Hospital, The Chinese University of Hong Kong, Shatin, NT, Hong Kong SAR, China  
 Tel: (852) 2632 3339  
 Fax: (852) 2647 3227  
 Email: waichichan@cuhk.edu.hk

## Introduction

Multi-drug-resistant tuberculosis (MDR-TB) strains are less contagious than their drug-sensitive counterparts,<sup>1,2</sup> based on the perception that mutations conferring drug resistance deleteriously affect the normal physiological functions of the pathogen. Drug-resistant mutants are expected to grow more slowly and/or exhibit milder virulence. This is known as the 'fitness cost' of drug resistance.<sup>3</sup> This may confine the frequency and seriousness of infections caused by drug-resistant pathogens. However, mutations in *Mycobacterium tuberculosis* (MTB) do not always result in loss of fitness.<sup>3</sup> Reduction in fitness of the pathogen can be restored by compensatory mutations in the genome,<sup>4</sup> hence MDR-TB strains can be as infectious and invasive as the drug-sensitive, non-mutated form.

This study aimed to determine the physiological fitness of MDR-TB isolates in Hong Kong by evaluating their infectivity and virulence. First, whether the target gene mutations suppressed the growth fitness of the organisms was determined. Second, the relative virulence of selected MTB isolates was assessed in terms of their ability to survive and replicate within macrophages. Third, the proteomic profiles of selected MDR-TB isolates were studied to determine whether drug-resistant organisms undergo significant physiological changes to compensate for the effects of resistance gene mutations.

## Methods

This study was conducted from January 2007 to December 2008. The growth rate of 88 selected MDR-TB strains was measured using the BBL Mycobacteria Growth Indicator Tube (MGIT) and the BACTEC MGIT 960 system. A fluorescent sensor sensitive to quenching by dissolved oxygen was used. Bacterial growth consumes oxygen and therefore enables the sensor to fluoresce, producing growth signals. Equal-sized populations of drug-resistant and drug-susceptible strains were inoculated in parallel into separate tubes and then incubated in BACTEC MGIT 960 for up to 2 weeks. Fluorescence changes during this period were recorded and the growth rate of each test strain was measured by recording the time required to produce an arbitrary breakpoint value in growth signal.

The human macrophage-like cells were derived from phorbol-ester-activated THP1 cells. Eight selected MTB strains of different resistance phenotypes were mixed with human macrophages at a ratio of one to ten bacterial cells to one macrophage in a well of a 24-well plate. After overnight incubation, the non-phagocytosed MTB cells were removed by filtration. The macrophages were lysed at day 4 and 7 to determine the number of viable MTB organisms recoverable to determine their ability to survive or replicate inside the macrophages. The data were compared to those of drug-sensitive organisms.

Total proteins were prepared for eight selected MTB strains that exhibited specific drug-resistance phenotypic patterns, followed by simultaneous analysis by two-dimensional gel electrophoresis alongside with drug-sensitive strains. Comparison of the proteomic profiles pinpointed proteins that were expressed specifically in either drug-resistant or -sensitive strains. Technically, total protein prepared from each strain was resolved on Bio-Rad Proteome

Works two-dimensional gel electrophoresis system. After electrophoresis, the gel was stained and scanned to produce a proteomic profile, which was analysed using the software provided by the manufacturer.

## Results

### Analysis of mycobacterial growth

In a preliminary attempt to assess the fitness cost of resistance gene mutations in MDR-TB isolates, the in vitro growth rate of 59 selected isolates with known drug susceptibility and genetic profiles were measured by recording the mean time required to reach a breakpoint value of 200 signal units in the MGIT system. To examine the correlation between growth rate and the number of mutations in the resistance genes, mutation profiles of the fastest and slowest growing strains were compared. The eight fastest-growing strains took a mean of 3.06 days to reach 200 signal units, and harboured two or fewer mutations. In contrast, the eight slowest-growing strains took a mean of 5.41 days to produce 200 signal units, and harboured at least three mutations (Table 1). Seven of these strains contained *gyrA* mutations, and five contained *pncA* mutations. Regarding the effect of mutations in specific resistance genes, wild-type strains required a mean of 3.58 days to produce 200 signal units, whereas the mean time taken by isolates containing mutations was much longer, ranging from 4.52 days for strains containing *katG* mutations to 4.91 days for strains containing *gyrA* mutations (Table 2). Strains carrying mutations in *gyrA* and *pncA*, with or without mutations in other genes, were the slowest-growing organisms, taking 4.91 and 4.83 days, respectively, to produce the reporter signal. The effects of mutations in specific genes were depicted by the growth rate in single mutants (Table 2). The mean time for strains harbouring a single mutation in *rpoB*, *embB*, and *katG* was 3.75, 4, and 4.36 days, respectively. Single mutants of the *gyrA* and *pncA* genes were not available for analysis.

To test whether mutation-induced fitness cost can attenuate the ability of MDR-TB to spread between human hosts, the growth rate of organisms that had been isolated from unrelated individuals and yet displayed almost identical genetic and drug-resistance profiles were measured (Table 3). The recovery of genetically identical organisms from up to 10 unrelated patients provided evidence that they possessed the ability to survive in human hosts and spread in the community. As these organisms also exhibited resistance to multiple antibiotics, we speculated that their survival fitness and hence infectivity might also be constrained by mutation-induced fitness cost to some extent. Measurement of the in vitro growth capacity of these organisms was therefore expected to reveal the actual impact of such fitness cost on the infectivity of MDR-TB organisms. Most of the 29 cluster isolates exhibited a significantly slower growth rate than did the drug-sensitive controls and other genetically diverse MDR-TB strains. Nevertheless, upon prolonged incubation, significant

growth was recorded for these cluster strains that eventually produce a population size comparable to that of other MDR-TB organisms.

### Mycobacterial survival fitness in macrophages

An intracellular survival assay was used to assess the in vivo fitness and virulence of eight selected drug-resistant MTB strains. The number of organisms taken up by macrophages was the difference between the viable cell counts before and after ingestion by macrophages. The numbers of viable organisms collected from washing the macrophage pellet as well as from lysis of the macrophage population at different time points after the ingestion step were recorded. A formula was derived to calculate the survival rate of MTB in macrophages (Table 4).

Drug-resistant MTB isolates generally exhibited reduced survival fitness when compared to drug-sensitive strains, which did not harbour mutations; such reduction was more apparent in the long term (day 7). Table 4 shows the relative survival rate of a wild-type strain (25117), a drug-sensitive clinical isolate (B8), and a representative multi-drug-resistant strain which contained mutations in five resistance

**Table 1. The mean initial growth rate of the fastest and slowest growing Mycobacterium tuberculosis isolates**

Strain no.	Resistance gene mutations involved	Mean initial growth rate (days to reach 00 signal units)
Fastest-growing strains		
M12	<i>embB</i> , <i>katG</i>	3
M14	<i>rpoB</i> , <i>katG</i>	3
M16	<i>rpoB</i>	3
M48	<i>rpoB</i>	3.5
M58	<i>rpoB</i> , <i>embB</i>	3
188a	-	3
417a	-	3
B7	-	3
lowest-growing strains		
M1	<i>rpoB</i> , <i>embB</i> , <i>katG</i>	5.5
M15	<i>rpoB</i> , <i>embB</i> , <i>pncA</i>	5.3
M29	<i>gyrA</i> , <i>rpoB</i> , <i>embB</i> , <i>katG</i>	5.35
M96	<i>gyrA</i> , <i>rpoB</i> , <i>embB</i> , <i>katG</i> , <i>pncA</i>	5.43
484	<i>gyrA</i> , <i>rpoB</i> , <i>embB</i> , <i>pncA</i>	5.32
G53211	<i>gyrA</i> , <i>rpoB</i> , <i>embB</i> , <i>pncA</i>	5.6
c1	<i>gyrA</i> , <i>rpoB</i> , <i>embB</i> , <i>pncA</i>	5.32
Y777	<i>gyrA</i> , <i>rpoB</i> , <i>embB</i> , <i>pncA</i>	5.43

**Table 2. Mean initial growth rate of isolates harbouring mutations in specific genes, with or without further mutations in other genes**

Resistance gene	Mean initial growth rate (days to reach 00 signal units)
No mutation (n=6)	3.58
<i>rpoB</i> (single mutant, n=4)	3.75
<i>katG</i> (single mutant, n=7)	4.36
<i>embB</i> (single mutant, n=1)	4.0
<i>rpoB</i> (multiple mutant, n=50)	5.59
<i>katG</i> (multiple mutant, n=29)	4.52
<i>embB</i> (multiple mutant, n=39)	4.59
<i>gyrA</i> (multiple mutant, n=24)	4.91
<i>pncA</i> (multiple mutant, n=26)	4.83

**Table 3. Mean initial growth rate and drug susceptibility profiles of 29 genetically related multi-drug-resistant *Mycobacterium tuberculosis* isolates**

Cluster/strain no.	Minimal inhibitory concentration of					Mean initial growth rate (days to reach 00 signal units)
	Ofloxacin	Rifampicin	Ethambutol	Isoniazid	Pyrazinamide	
C9-1	0.6/S	>64/R	2/S	1/R	50/S	9.4
C9-2	1.2/S	>64/R	2.8/S	1/R	50/S	11.5
C9-3	1.2/S	>64/R	2.8/S	1/R	50/S	9.0
C9-4	0.6/S	>64/R	2/S	1/R	50/S	9.4
C9-5	0.6/S	>64/R	2/S	1/R	50/S	8.3
C9-6	0.6/S	>64/R	2/S	1/R	50/S	9.0
C17-1	1.2/S	>64/R	2/S	>1/R	-	9.0
C17-2	1.2/S	>64/R	2/S	1/R	-	9.4
C17-3	1.2/S	64/R	2/S	>1/R	-	9.4
C17-4	0.6/S	>64/R	2/S	>1/R	50/S	9.6
C17-5	1.2/S	64/R	2/S	>1/R	50/S	8.7
C17-6	1.2/S	64/R	2/S	>1/R	50/S	8.8
C22-1	1.2/S	>64/R	2.8/S	1/R	50/S	9.8
C22-2	2.4/S	>64/R	>4/R	>1/R	>50/R	9.0
C22-3	>4.8/R	>64/R	4/R	1/R	>50/R	8.6
C22-4	>4.8/R	>64/R	4/R	1/R	-	5.2
C33-1	1.2/S	>64/R	2.8/S	>1/R	50/S	9.5
C33-2	>4.8/R	>64/R	>4/R	>1/R	>50/R	8.8
C33-3	>4.8/R	>64/R	>4/R	1/R	>50/R	8.9
C33-4	>4.8/R	>64/R	>4/R	1/R	>50/R	9.0
C33-5	>4.8/R	>64/R	>4/R	1/R	>50/R	9.1
C33-6	>4.8/R	>64/R	>4/R	1/R	>50/R	4.5
C39-1	2.4/S	>64/R	4/R	1/R	50/S	9.3
C39-2	>4.8/R	>64/R	>4/R	>1/R	-	9.5
C39-3	4.8/R	>64/R	>4/R	1/R	-	12.8
C39-4	2.4/S	>64/R	>4/R	1/R	>50/R	9.4
C39-5	4.8/R	>64/R	4/R	1/R	>50/R	10.7
C39-6	2.4/S	>64/R	>4/R	1/R	>50/R	5.4
C39-7	4.8/R	>64/R	4/R	1/R	>50/R	5.7
188a*	1.2/S	16/S	2/S	0.2/S	-	3.0
417a*	1.2/S	16/S	2/S	1/S	-	3.0

\* Drug-sensitive strain as controls

**Table 4. Intracellular survival rate of *Mycobacterium tuberculosis* (MTB) in macrophages**

Calculation of intracellular survival rate*	25117 (wild-type strain)		B8 (drug-sensitive strain)		M96 (multi-drug-resistant strain)	
	Day 4	Day 7	Day 4	Day 7	Day 4	Day 7
VCLP	4x10 <sup>4</sup>	3x10 <sup>4</sup>	1.2x10 <sup>2</sup>	1.8x10 <sup>2</sup>	4x10 <sup>4</sup>	3x10 <sup>4</sup>
VCULP	2x10 <sup>4</sup>	1.3x10 <sup>3</sup>	50	20	3x10 <sup>4</sup>	4x10 <sup>3</sup>
VCI	2.5x10 <sup>5</sup>	1.6x10 <sup>6</sup>	3x10 <sup>4</sup>	3x10 <sup>5</sup>	3x10 <sup>6</sup>	2x10 <sup>7</sup>
VCUT	1x10 <sup>4</sup>	6x10 <sup>4</sup>	30	500	3x10 <sup>4</sup>	6x10 <sup>4</sup>
VCLP-VCULP	2x10 <sup>4</sup>	2.87x10 <sup>4</sup>	70	3.6x10 <sup>3</sup>	1x10 <sup>4</sup>	2.6x10 <sup>4</sup>
VCI-VCUT	2.4x10 <sup>5</sup>	1x10 <sup>5</sup>	3x10 <sup>4</sup>	3x10 <sup>5</sup>	3x10 <sup>6</sup>	2x10 <sup>7</sup>
(VCLP-VCULP)/(VCI-VCUT)	8.3%	28.7%	0.2%	1.2%	0.3%	0.13%

\* VCLP denotes viable count obtained after plating out a lysed macrophage pellet without washing, VCULP viable count obtained after plating out wash fluid collected from washing a macrophage pellet, VCI the initial viable count prior to macrophage uptake, and VCUT viable count of remaining free MTB after the macrophage uptake step. Hence, (VCLP-VCULP) depicts the number of organisms that survived intracellular stress, and (VCI-VCUT) depicts the number of organisms taken up by macrophages. Noted that the macrophage pellet might contain extracellular MTB which were neither ingested by macrophages nor eradicated by antibiotic or filtration

genes (M96) in macrophages 4 and 7 days after inoculation and uptake by macrophages. The survival rate of the wild-type strain in macrophages was much higher than that of the clinical isolates, regardless of whether they harboured mutations. At day 4, both clinical isolates tested exhibited a survival rate of less than 1%, whereas that of the wild-type strain (strain 25117) was 8%. At day 7, strains 25117 and B8, both harbouring wild-type nucleotide sequences in the resistance genes, displayed a higher cell count than that of day 4. This suggests that intracellular organisms regained growth fitness during the intervening period. In contrast, the viability count of strain M96, which harboured multiple

mutations in five resistance genes (*rpoB*, *katG*, *embB*, *gyrA*, and *pncA*) declined during this period. This indicates that mutation bearing organisms were less fit to survive macrophage-induced intracellular stress. Nevertheless, a small number of viable cells were still recoverable.

#### **Proteomic analysis of drug-resistant strains**

To determine whether drug-resistant isolates undergo significant physiological changes to accommodate the structural changes imposed by drug-resistance gene mutations, preliminary proteomic analyses on MDR-TB strains that harboured mutations in up to five drug-

resistance genes were performed. The MDR-TB isolates exhibited a small but discernable difference in proteomic profiles when compared to the drug-sensitive strains. Further experiments are necessary to confirm whether drug-resistance development involves physiological changes other than those concerning the drug target functions.

## Discussion

Drug target gene mutations in MTB conferred drug resistance at the expense of physiological fitness of the pathogen, rendering them less capable of multiplying even in a nutrient-rich environment. Isolates containing mutations in *gyrA* experienced the strongest growth inhibition. However, since these isolates also harboured mutations in other resistance genes, we could only indirectly assess the relative impact of *gyrA* mutations on growth inhibition by comparing the effects of single mutations in other resistance genes. Mutations in *rpoB* or *katG*, the two genes involved in resistance to the first-line drugs rifampicin and isoniazid, exhibited weaker growth retardation than multiple mutations. The significant growth inhibition phenomenon observed in multiple mutants was attributed to additional *gyrA* mutations. Structural alteration of gyrase is expected to affect the efficiency of DNA and cellular replication, leading to a slower growth rate. The fact that isolates that harboured a single mutation in the *rpoB* gene exhibited a growth rate similar to that of wild-type strains indicated that RNA polymerase, the *rpoB* gene product, was more flexible in accommodating mutation-directed structural changes. In contrast, isolates carrying mutations in the *katG* gene grew much slower. This suggested that the *katG* gene product played an important role in defending against oxidative stress during the growth process when reactive oxygen species were being produced.

Despite a reduced initial growth rate, all tested mutants eventually grew to a population size comparable to that of the wild type. This suggested that the growth fitness cost of resistance-gene mutations only slowed down mycobacterial growth at the initial phase immediately after inoculation, possibly with little negative effect on the overall ability to cause disease in human hosts. The growth fitness data on clonal MDR-TB strains also suggested that a severe growth fitness cost did not necessarily hamper the ability of the organism to infect humans and survive. In addition to the mutation-induced effects, growth and survival fitness of MDR-TB was also highly dependent on the overall genetic constraints, which are unique to each organism. The nature

of constraint factors other than those in drug-resistance genes has yet to be determined. This finding is alarming as it indicates that MDR-TB mutants are fully capable of residing in human host-reservoirs and are as effective as their non-resistant counterparts in causing infections in the community.

In addition, MDR-TB strains were also found to exhibit reduced survival fitness, especially in the long term, after they had been engulfed in macrophages. Reduced survival of resistant MTB strains was likely to be due to their impaired ability to produce stress responses as a result of genetic mutations in resistance genes. *katG* is likely to be a major candidate gene which contributes to intracellular survival by producing catalase-mediated antioxidant responses against the detrimental effects of reactive oxygen species produced by macrophages. Other drug-resistance genes may also affect survival fitness indirectly. For example, mutations in the *embB* gene affect cell wall integrity, leading to a weaker structure that is less resistant to oxidative stress in the intracellular compartment of macrophages.

Resistance-gene mutations could cause detectable changes in proteomic profiles, indicating that they elicited secondary or compensatory changes in the physiology of the resistant strains. Our study revealed the effects of the fitness costs of resistance gene mutations on the infectivity and virulence of MDR-TB organisms. Such data should facilitate development of novel strategies for the control of this important pathogen.

## Acknowledgement

This study was supported by the Research Fund for the Control of Infectious Diseases, Food and Health Bureau, Hong Kong SAR Government (#06060132).

## References

1. Ormerod LP. Multidrug-resistant tuberculosis (MDR-TB): epidemiology, prevention and treatment. *Br Med Bull* 2005;73-74:17-24.
2. Raviglione MC, Gupta R, Dye CM, Espinal MA. The burden of drug-resistant tuberculosis and mechanisms for its control. *Ann N Y Acad Sci* 2001;953:88-97.
3. Sander P, Springer B, Prammananan T, et al. Fitness cost of chromosomal drug resistance-conferring mutations. *Antimicrob Agents Chemother* 2002;46:1204-11.
4. Bottger EC, Springer B, Pletschette M, Sander P. Fitness of antibiotic-resistant microorganisms and compensatory mutations. *Nat Med* 1998;4:1343-4.

ETY Leung 梁東耀  
M Ip 葉碧瑤  
EWC Chan 陳維智  
RCY Chan 陳超揚

# A real-time polymerase chain reaction protocol for rapid detection of *Mycobacterium tuberculosis*, drug resistance, and Beijing genotype

## Key Messages

1. DNA extraction methods enable molecular detection of *Mycobacterium tuberculosis* (MTB) from sputum specimens.
2. A sensitive and specific multiplex real-time polymerase chain reaction assay enables simultaneous detection of MTB, isoniazid and rifampin resistance, and Beijing/W genotype.
3. Molecular diagnosis of MTB greatly reduces the turnaround time of conventional culture methods.

## Introduction

The emergence of multidrug-resistant and extensive-drug-resistant tuberculosis (TB) is a major challenge worldwide. Recent clinical and epidemiological implications have highlighted the virulence of the Beijing/W genotype of *Mycobacterium tuberculosis* (MTB).<sup>1,2</sup> Development of fast and reliable methods for diagnosis and molecular characterisation of MTB is essential to its effective control. Conventional culture and antimicrobial tests require 6 to 8 weeks to obtain the results. Beijing genotyping by traditional *IS6110*-fingerprinting takes a further 3 days after the culture is obtained. Rapid detection of MTB using commercial diagnostic systems is limited by their costs and/or their requirement of specific equipment. About 81% of rifampin resistance (RIF<sup>R</sup>) and 77.5% of isoniazid resistance (INH<sup>R</sup>) are caused by point mutations in *rpoB*, *katG*, *mabA* genes.<sup>3-5</sup> Genomic regions of difference can be used for differentiation of Beijing and non-Beijing genotypes.<sup>2</sup> This study aimed to develop a single real-time polymerase chain reaction (PCR) assay for the diagnosis of MTB, detection of INH and RIF resistance, and detection of Beijing/W genotypes.

## Methods

This study was conducted from January 2009 to July 2010. A collection of *M. tuberculosis* H37Rv, *M. bovis*, and 17 reference strains of non-tuberculosis mycobacteria (NTM) from the American Type Culture Collection were used for validation of primer specificities. In addition, 80 clinical isolates of *M. tuberculosis* (20 Beijing/W, 20 non-Beijing/W, 20 INH<sup>R</sup>, 20 RIF<sup>R</sup>) were collected from Hong Kong during 2004 to 2009. The phenotypes and genotypes were confirmed by minimum inhibitory concentration and deletion-targeted multiplex PCR, respectively.<sup>2</sup>

Specimens were collected for comparison of DNA extraction methods and evaluation of the assay. A total of 3012 non-duplicate sputum specimens were collected from the clinical microbiology laboratory of the Prince of Wales Hospital during January 2009 to April 2010. Of them, 60 were acid-fast bacilli (AFB) smear positive and 275 were from patients with strong clinical features of TB or with severe pulmonary infection. These 335 specimens were selected for evaluation of the assay.

To enable high sensitivity for the detection of MTB nucleic acids directly from sputum, the protocol for bacterial nucleic acid extraction was optimised by evaluating three different beads for mechanical cell lysis; and four different downstream DNA purification methods for a total of 12 protocols. Three different beads included 0.1 mm zirconia beads (BioSpec Products), 0.2 mm glass beads, and 1 mm glass beads (Sigma Aldrich). After mechanical disruption, the lysate was subjected to DNA purifications using four different methods, including Dynabeads MyOne SILANE magnetic beads (Invitrogen), QIAmpMinElute Virus spin kit, QIAmp DNA Mini Kit (Qiagen), and Chelex 100 resins (Bio-Rad Laboratories). Both spiked sputum and clinical specimens were used for evaluation of extraction methods; 2 mL aliquots of spiked sputum or clinical

Hong Kong Med J 2013;19(Suppl 5):S8-11

Department of Microbiology, The Chinese University of Hong Kong  
ETY Leung, M Ip, EWC Chan, RCY Chan

RFICD project number: 08070212

Principal applicant and corresponding author:  
Dr Eric Tung-Yiu Leung  
Department of Microbiology, The Chinese University of Hong Kong, Prince of Wales Hospital, Shatin, New Territories, Hong Kong SAR, China  
Tel: (852) 2632 2573  
Fax: (852) 2647 3227  
Email: ericleung@cuhk.edu.hk

sputum specimens (nine AFB smear positive and eight AFB smear negative) were centrifuged and the pellet was resuspended with 1 mL of TE buffer. Mechanical cell lysis was performed in a Disruptor Genie (Scientific Industries). The lysates were incubated at 95°C for 10 minutes for complete inactivation of the bacteria, and 100 µL aliquots of the lysates were used for DNA purification. With Chelex resins, the lysate was added to an equal volume of 10% Chelex 100 resins and incubated at room temperature for 5 minutes with occasional mixing. The mixture was centrifuged to collect the supernatant, which was directly used as DNA templates for real-time PCR. Other methods were performed according to the manufacturer's recommendation and eluted in a final volume of 30 µL. The buffers for Invitrogen magnetic beads were prepared in-house as previously described,<sup>1,6</sup> with slight modification on the wash buffer. Wash buffer was prepared by combining 55 mL of ethanol and 45 mL of solution containing 3M guanidiniumthiocyanate, 10 mM Tris-HCl, and 10 mM NaCl at a pH of 8.0.

Regarding development of multi-probe multiplex real-time PCR, various gene-specific primers and probes were designed and tested with our collection of strains for verification of specificities (Table 1). Amplification of human β-globin gene by primers HB-F and HB-R acted as internal amplification controls to identify PCR inhibition. Real-time PCR was undertaken in triplicate wells in an Applied Biosystems 7700 real-time PCR instrument. For comparison of MTB extraction methods, each well contained 25 µL of reaction volume, including 12.5 µL of Taqman Universal Master Mix, 500 nM of MTB-F, 300 nM of MTB-R, 50 nM of MTB-P, and 2.5 µL of DNA extracts. For evaluation of the final assay with 335 clinical specimens, the 25 µL of reaction volume also contains

600 nM of BJW-F, 900 nM of BJW-R, 80 nM of BJW-P, 50 nM of HB-F, 30 nM of HB-R, and 50 nM of HB-P in addition. The instrument was programmed to 95°C for 10 minutes, and 40 cycles of 95°C for 15 seconds and 60°C for 1 minute. Positive specimens were subsequently subjected to resistance detection in two real-time PCR reactions. One reaction contained 12.5 µL of Taqman Universal Master Mix, 100 nM of KatG-F, 100 nM of KatG-R, 50 nM of KatG-P, 50 nM of RpoB-F, 50 nM of RpoB-R, 50 nM of RpoB-P526, and 2.5 µL of DNA extracts in a 25 µL reaction volume. The other reaction contained 12.5 µL of Taqman Universal Master Mix, 100 nM of MABA-F, 80 nM of MABA-R, 50 nM of MABA-P, 50 nM of RpoB-F, 50 nM of RpoB-R, 50 nM of RpoB-P531, and 2.5 µL of DNA extracts in a 25 µL reaction volume. Both reactions were subjected to 95°C for 10 minutes, 40 cycles at 95°C for 15 second and 61°C for 1 minute. Control DNA extracts from H37Rv and the sequenced INH<sup>R</sup> and RIF<sup>R</sup> control strains were used in each run.

## Results

### Comparison of DNA extraction methods

With both spiked and clinical specimens, zirconia beads in combination with magnetic beads (or with spin columns) consistently produced the lowest Ct values (highest yield of DNA). Taking into consideration the sensitivity, the simplicity of protocol and the potential for automation, the combination of zirconia beads and magnetic beads was selected.

### Evaluation of the developed extraction and real-time PCR protocol

End-point detection limits of the real-time PCR for MTB detection and Beijing/W detection were 5 and 50 fg of MTB

**Table 1. Primers and probes for real-time polymerase chain reaction**

Gene target (amplification size [bp])	Primers and probes	Sequence (5' --> 3')
<i>IS6110</i> (133)	MTB-F	5'-GCCGGATCAGCGATCGT-3'
	MTB-R	5'-GCAAAGTGTGGCTAACCCTGAA-3'
	MTB-P	5'-FAM-TTCGACGGTGCATCTG-3'-MGB
<i>Rv0927c - pstS3</i> intergenic region (75)	BJW-F	5'-ATGCACGGCATAACGGACAT-3'
	BJW-R	5'-GGTTGACCCCTGATGATGGAC-3'
	BJW-P	5'-NED-TGAGATCCGCGGTCG-3'-MGB
Human β-globin (115)	HB-F	5'-TTCTGACACAACCTGTGTTCACTAGC-3'
	HB-R	5'-CAACTTCATCCACGTTCCACC-3'
	HB-P	5'-VIC-CTCCTGAGGAGAAGTC-3'-MGB
Catalase peroxidase (122)	KATG-F	5'CCGTACAGGATCTCGAGGAAACT-3'
	KATG-R	5'TTGGGCTGGAAGAGCTCGTAT-3'
	KATG-P	5'-NED- CGATGCCGGTGGTGA-3'-MGB
Promoter region of <i>mabA</i> gene (119)	MABA-F	5'-CACGTTACGCTCGTGGACATAC-3'
	MABA-R	5'-CAGGACTGAACGGGATACGAAT-3'
	MABA-P	5'-FAM-CAACCTATCATCTCGC-3'-MGB
RNA polymerase B subunit (166)	RPOB-F	5'-ACCGCAGACGTTGATCAACAT-3'
	RPOB-R	5'-GGCAGCTCACGTGACAG-3'
	RPOB-P526	5'-VIC-CGCTTGTMGGTCAAC-3'-MGB
	RPOB-P531	5'-VIC- AGCGCCAACAGTC-3'-MGB

DNA, respectively, which correspond to approximately one and 10 bacilli. Of 335 specimens tested using the zirconia beads plus the magnetic beads protocol, 74 were MTB culture-positive, 31 were NTM culture-positive, and 230 were culture-negative for mycobacterium (Table 2). Of the 335 specimens, 89 (26.6%) were positive for MTB by real-time PCR. All MTB culture-positive specimens were positive by real-time PCR. Fifteen culture-negative specimens, including five AFB smear-positive and 10 AFB smear-negative, were positive by real-time PCR. Among these 15 specimens, 12 came from patients diagnosed with TB and three from subjects with a TB history. None of the NTM culture-positive specimens were positive for MTB by real-time PCR. Taking conventional culture as the gold standard, the overall sensitivity and specificity were 100% (74/74) and 94.3% (246/261), respectively. Taking into account the clinical diagnosis of the patients, the specificity was 100% (246/246). Associations of Beijing/W genotypes with AFB smear-positive and smear-negative specimens were 59.6% (31/52) and 21.6% (8/37), respectively. Inhibition of amplification was not encountered as determined by internal positive controls. Of the 89 positive specimens, two with RpoB 531 mutations (RIF<sup>R</sup>) and KatG 315 mutations (INH<sup>R</sup>) were identified. One specimen with a MabA promoter mutation (INH<sup>R</sup>) was also identified. The results concord with minimum inhibitory concentration results after isolation of the strains. Sensitivities for RIF<sup>R</sup> and INH<sup>R</sup> with clinical specimens were thus 100% (2/2) and 50% (3/6), respectively. End-point detection limits of the

real-time PCR for INH<sup>R</sup> and RIF<sup>R</sup> were 250 fg (~50 bacilli).

## Discussion

Sensitive detection of MTB from bodily fluids requires optimal cell lysis and efficient DNA purification to remove associated PCR inhibitors. It is challenging for these two steps to be well-accomplished in sputum specimens, owing to the thick durable bacterial cell wall, the uneven distribution of cells in the fluid due to high tendency of clumping, the abundance of PCR inhibitors in sputum, and most of the time a minute amount of MTB DNA quenched by rich human DNA background. The choice of reagents and methods greatly affects the DNA yield and hence the sensitivity of an assay.

Our novel multi-probe multiplex real-time PCR successfully detected all 74 cultivable MTB isolates with no cross reaction with NTM. Fifteen specimens that were PCR positive were culture negative. Considering the clinical diagnosis of the patients, the chance of false positivity is low. Since PCR could detect nucleic acids from nonviable MTB (due to treatment) or viable MTB in insufficient numbers for successful culture, this may be an advantage over conventional cultures. With the 80 collected isolates, 75% of INH<sup>R</sup> (15/20) and 70% of RIF<sup>R</sup> (14/20) could be detected by our real-time PCR. The remaining portions did not confer resistance by katG-315 or RpoB-526/531 mechanisms, as confirmed by DNA sequencing.

**Table 2. Sensitivities and specificities of real-time polymerase chain reaction (PCR) in reference to conventional culture**

Respiratory specimens (n=335)	No. of detection by real-time PCR			
	<i>Mycobacterium tuberculosis</i> (MTB)	Beijing/W	Isoniazid resistance (n=6)	Rifampin resistance (n=2)
MTB culture-positive (n=74)				
Smear-positive (n=47)	47	28	1	1
Smear-negative (n=27)	27	6	2	1
Non-tuberculosis mycobacteria culture-positive (n=31)*				
Smear-positive (n=7)	0	-	-	-
Smear-negative (n=24)	0	-	-	-
Culture-negative for <i>Mycobacterium</i> (n=230)				
Smear-positive (n=6)	5 <sup>†</sup>	3	0	0
Smear-negative (n=224)	10 <sup>‡</sup>	2	0	0

\* Including *M. avium* (n=7), *M. chelonae* (n=6), *M. fortuitum* (n=6), *M. goodii* (n=1), *M. kansasii* (n=4), *M. neoaurum* (n=2), *M. simiae* (n=1), *M. terrae* (n=1), and *Mycobacterium runyon* group III (n=3)

<sup>†</sup> Including four patients with other sputum specimens positive for MTB (by culture) and one patient with confirmed TB (by histology)

<sup>‡</sup> Including six patients with other sputum specimens positive for MTB (by culture), three patients with a recent TB history, and one patient with confirmed TB (by histology)

**Table 3. Comparison of conventional *Mycobacterium tuberculosis* (MTB) culture and the molecular protocol**

Parameter	Conventional MTB culture	Molecular protocol
Throughput	Single specimen, manually	Automatically in 96 well formats
Turnaround time	6-8 weeks	<4 hours
Labour	20 min/10 specimens	~40 min/10 specimens (manual operation)
Space/equipment	Biosafety Level III laboratory, Class II biological safety cabinet, warm room for 8-week incubation	Biosafety Level II laboratory, Class II biological safety cabinet for DNA extraction, separate room for master mix preparation, real-time polymerase chain reaction (PCR) machine
Costs of reagents	HK\$10*/specimen	HK\$35 <sup>†</sup> /specimen

\* Including two Lowenstein-Jensen culture; additional HK\$35 for Isoniazid and Rifampin resistance detection.

<sup>†</sup> Including zirconia beads, buffers, magnetic beads, and PCR reagents

With clinical specimens, three out of six INH<sup>R</sup> specimens and two out of two RIF<sup>R</sup> specimens were identified.

Contrasting conventional MTB culture with the molecular protocol was described. The latter greatly reduced the turnaround time, which was beneficial to both TB control and to patients (Table 3). It also avoided the hazards of maintaining a TB culture room. However, the molecular protocol is more labour intensive than conventional cultures, unless automation is available. Though the cost of this protocol is significantly lower than commercially available rapid TB diagnosis systems, the cost of reagents is nevertheless higher than conventional culture, which could still be a barrier for its use. As the cost of molecular reagents drops, in the foreseeable future the cost of molecular methods may become reasonable for epidemiological and health care purposes. In conclusion, a new optimised molecular protocol was successfully developed for simultaneous detection of MTB, resistance and Beijing/W genotype, with high sensitivity and specificity.

### Acknowledgements

This study was supported by the Research Fund for the Control of Infectious Diseases, Food and Health Bureau, Hong Kong SAR Government (#08070212). We thank Dr

Raymond Lai and Mr WY Lau of the clinical microbiology laboratory, Prince of Wales Hospital, for their assistance in specimen collection. We also thank the administrators and technicians of the BSL3 Laboratory, Li Ka Shing Institute of Health Sciences, The Chinese University of Hong Kong for their advice and support.

### References

1. Ebrahimi-Rad M, Bifani P, Martin C, et al. Mutations in putative mutator genes of *Mycobacterium tuberculosis* strains of the W-Beijing family. *Emerg Infect Dis* 2003;9:838-45.
2. Chen J, Tzolaki AG, Shen X, Jiang X, Mei J, Gao Q. Deletion-targeted multiplex PCR (DTM-PCR) for identification of Beijing/W genotypes of *Mycobacterium tuberculosis*. *Tuberculosis (Edinb)* 2007;87:446-9.
3. Yam WC, Tam CM, Leung CC, et al. Direct detection of rifampin-resistant *Mycobacterium tuberculosis* in respiratory specimens by PCR-DNA sequencing. *J Clin Microbiol* 2004;42:4438-43.
4. Leung ET, Ho PL, Yuen KY, et al. Molecular characterization of isoniazid resistance in *Mycobacterium tuberculosis*: identification of a novel mutation in *inhA*. *Antimicrob Agents Chemother* 2006;50:1075-8.
5. Leung ET, Kam KM, Chiu A, et al. Detection of *katG* Ser315Thr substitution in respiratory specimens from patients with isoniazid-resistant *Mycobacterium tuberculosis* using PCR-RFLP. *J Med Microbiol* 2003;52:999-1003.
6. Boom R, Sol CJ, Salimans MM, Jansen CL, Wertheim-van Dillen PM, van der Noordaa J. Rapid and simple method for purification of nucleic acids. *J Clin Microbiol* 1990;28:495-503.

SKW Tsui 徐國榮  
 RCY Chan 陳超揚  
 KM Kam 甘啟文  
 HS Kwan 關海山  
 KS Leung 梁廣錫  
 KP Fung 馮國培  
 MMY Waye 韋妙宜  
 PTW Law 羅迪雲  
 SK Lou 婁紹科  
 KK Leung 梁家傑

# Genome analysis of *Mycobacterium tuberculosis* Beijing family strains

.....

## Introduction

*Mycobacterium tuberculosis* (MTB) currently affects more than two billion people and causes 1.5 to 2 million deaths every year. Multidrug-resistant and the virtually untreatable extensively drug-resistant MTB strains are estimated to cause 490 000 and 40 000 new cases per year, respectively. A Beijing/W subtype has attracted attention for its global emergence, increased transmissibility, and tendency to develop multidrug resistance. In the Beijing/W strain, alterations in DNA repair genes, *mutT2*, *mutT4*, and *ogt*, result in increased mutation frequencies and better adaptability to stress. Compared with *Mycobacterium bovis* and H37Rv, the Beijing/W subtype has an intact open reading frame of *pks15/1*, which is involved in the biosynthesis of phenolic glycolipids and may contribute to its hypervirulence. The Beijing/W subtype has three unique classes of large sequence polymorphisms (LSPs): four LSPs (RD105, RD149, RD152, and RD207) that are deleted; three LSPs (RD142, RD150, and RD181) that are variably deleted; and 14 LSPs that are encountered in individual isolates.

To understand the genetic factors responsible for the drug-resistant phenotype in the Beijing/W strains, we sequenced the genome of three isolates of MTB Beijing/W subtype, one of which was drug-sensitive and the other two were drug-resistant. The latter were resistant to nearly all commonly used anti-TB drugs, which we termed a 'totally drug-resistant' (TDR) phenotype. We compared the genome sequences of these three isolates with known MTB complete genome sequences having drug-resistant profiles.

## Methods

This study was conducted from September 2008 to August 2010. The genomes of the TDR strains, BT1 and BT2, and the drug-sensitive strain BS1 were sequenced using the Roche 454 GS FLX pyrosequencing system. Reference assembly was performed separately using the manufacturer-provided software (GS Mapper) as well as BWA. De novo assembly was also performed using Velvet. The two sets of scaffolds were then compared and combined to form a first draft, using our in-house scripts. Gaps closure was performed using the Sanger approach. Whole-genome sequence comparison and alignment were done in Mauve and Mummer.

Genome sequences were first annotated using an automated subsystem approach. Results were then carefully crosschecked with GLIMMER as well as search outputs from a non-redundant nucleotide database. Additional ontological information was obtained from KEGG. Phylogenetic analysis was conducted by comparing the four Beijing/W isolates to a set of 113 geographically diverse MTB isolates using polymorphic loci found within a set of 89 housekeeping genes. MEGA4 was used to generate a NJ tree.

For SNP analysis, the reference strains used were: H37Rv (RL123456.2), H37Ra (NC\_00952.1), KZN4207 (NZ\_ACVS00000000), KZN1435 (NC\_012943), and KZN605 (NZ\_ABGN00000000).<sup>1</sup>

The inter-relationship of mutated genes was studied by submitting the gene list to the DAVID Gene Functional Classification Tool, and also by the STRING software for the prediction of protein-protein interaction network.

## Key Messages

1. The genomes of the three 'totally drug-resistant' (TDR) Beijing/W strains of *Mycobacterium tuberculosis* (MTB) were sequenced and compared with publicly available genome sequences of KwaZulu-Natal MTB.
2. The sequences of the KwaZulu-Natal MTB strains shared a close ancestral relationship with MTB F11, whereas the three Beijing/W isolates formed a separate cluster.
3. The numbers of deletions, truncations, and frame-shift mutations were significantly greater in TDR Beijing/W strains.
4. Some DNA repair genes were defective in TDR Beijing/W strains.
5. Many genes involved in optimal mycobacterial growth were mutated in TDR Beijing/W strains.

Hong Kong Med J 2013;19(Suppl 5):S12-4

### The Chinese University of Hong Kong:

School of Biomedical Sciences

SKW Tsui, KP Fung, MMY Waye

Hong Kong Bioinformatics Centre

SKW Tsui, SK Lou, KK Leung

Centre for Microbial Genomics and Proteomics

SKW Tsui

Department of Microbiology

RCY Chan

School of Life Sciences

HS Kwan

Department of Computer Science and

Engineering

KS Leung

Faculty of Science

PTW Law

Public Health Laboratory Centre, Hospital

Authority

KM Kam

RFID project number: 08070502

Principal applicant and corresponding author:

Prof Stephen Kwok Wing Tsui

School of Biomedical Sciences, The Chinese

University of Hong Kong, Shatin, NT, Hong

Kong SAR, China

Tel: (852) 2609 6381

Fax: (852) 2603 7732

Email: kwtsui@cuhk.edu.hk

## Results

The three MTB Beijing/W isolates were obtained from the Tuberculosis Reference Laboratory at the Public Health Laboratory Centre of the Department of Health, Hong Kong Special Administrative Region. They were chosen based on: (1) their drug-resistance phenotypes, and (2) individual differences in RFLP patterns to maximise heterogeneity in genomic variations for comparison. The drug-sensitive strain, BS1, was sensitive to streptomycin, isoniazid, rifampicin, and ethambutol, whereas the two TDR strains, BT1 and BT2, were resistant to these antimicrobials as well as ethionamide, kanamycin, capreomycin, ofloxacin, amikacin, and pyrazinamide. The genomic DNA of the three isolates was extracted, purified, and subjected to high-throughput sequencing using the Roche 454 approach. The sequences of all the strains were then gap-filled and sequenced to completion. The three genomes were fully annotated and their corresponding GenBank files were submitted to the National Center for Biotechnology Information, National Institute of Health, USA. Whole-genome sequence alignment was performed. The genomic sequences of many KwaZulu-Natal (KZN) strains were publicly available. The phylogenetic relationships between the three Beijing/W isolates and the KZN strains, along with all the known MTB genomes were compared. The three KZN strains shared a close ancestral relationship with MTB F11, whereas the three Beijing/W isolates formed a separate cluster.

To identify novel genetic factors associated with the drug-resistance phenotype in the Beijing/W subtype, we identified genes that were frame-shifted, truncated, or lost, as well as non-synonymous SNPs that were specific in drug-resistant strains but not drug-sensitive strains. To reduce the number of false positives, we adopted more stringent criteria by excluding the hypermutable PPE proteins, PE-PGRS proteins, repetitive proteins, hypothetical proteins, proteins with synonymous substitution and mutations in promoter and intergenic regions. The numbers of mutations in Beijing/W drug-resistant strains were significantly greater than in other drug-resistant strains. Many of the mutations, such as those within haemolysin A, the TetR family transcriptional repressor, DNA gyrase subunit A, catalase-peroxidase and DNA-directed RNA polymerase subunit  $\beta$ , were present in our Beijing/W TDR isolates. However, mutations in these genes may differ in terms of amino acid changes and codon numbers when compared with reported mutation hot spots. Surprisingly, the number of deletions, truncations, and frame-shift mutations were significantly greater in TDR strains.

There were 15 genes that were common in the two BT strains. The overlap was small, which reflected the stochastic nature of the emergence of drug resistance or non-clonality (owing to the increased fitness cost associated with drug-resistance mutations). Among the commonly mutated genes in the two strains, only seven were associated with drug

resistance.

To explore the relationship of mutated genes, the gene list was submitted to the DAVID Gene Functional Classification Tool.<sup>2</sup> Significant enrichment of the mismatch repair, geraniol degradation, and nicotinate and nicotinamide metabolism pathways was identified. As none of the mutator phenotypes (mutT1, mutT2, and mutT3) in the Beijing/W strains had changes, other genes involved in the mismatch repair of MTB were examined.<sup>3</sup> Mutations were found in three DNA repair-related genes in BT1 and one in BT2. We hypothesised that the two BT strains weakened their mismatch repair machinery to enable more aggressive destructive evolution in order to survive the inhibition caused by a large number of anti-TB drugs.

Genes required for mycobacterial growth are defined by high-density mutagenesis.<sup>4</sup> A total of 614 genes were considered essential for optimal growth in MTB and *M bovis*. Among genes having a non-synonymous mutation in Beijing/W and KZN families, only one in each KZN strain and 12 and 10 in BT1 and BT2, respectively, were identified. The increased mutation rate of genes for optimal growth implies that MTB strains with extreme drug resistance tend to slow down their growth in order to survive. This is in line with the hypothesis that TDR MTB strains are rare because of the high fitness cost of developing drug resistance.

The STRING software was used to study the inter-relationship of genes with non-synonymous mutations.<sup>5</sup> A cluster of lipid metabolism-associated genes were found in the PPI network, and many novel gene products interacting with known drug targets were identified. These gene products may be related to the establishment and maintenance of the drug resistance. These products may modulate or compensate the mutations in the drug-resistant genes.

## Discussion

*M leprae* evolved from other mycobacterium species by reductive evolution. Only 1604 potentially active genes remain, 1439 of which can be found in MTB. The *M leprae* and TDR strains have many similar properties, including slow growth and gene decay by deletion and frame-shift. The dnaQ-mediated proofreading activities of DNA polymerase III is lost in *M leprae*, whereas mutations are detected in the Pol III in BT1. On comparing the list of deleted genes with the genes with non-synonymous mutations in BT1 and BT2, there are significant overlaps in the categories of fatty acid metabolism genes, lipid-related genes, esterase, and membrane proteins. We consider that TDR MTB strains follow the reductive evolution strategy of *M leprae*.

## Acknowledgement

This study was supported by the Research Fund for the

Control of Infectious Diseases, Food and Health Bureau, Hong Kong SAR Government (#08070502).

## References

1. Ioerger TR, Koo S, No EG, et al. Genome analysis of multi- and extensively-drug-resistant tuberculosis from KwaZulu-Natal, South Africa. *PLoS One* 2009;4:e7778.
2. Huang da W, Sherman BT, Tan Q, et al. The DAVID Gene Functional Classification Tool: a novel biological module-centric algorithm to functionally analyze large gene lists. *Genome Biol* 2007;8:R183.
3. Mizrahi V, Andersen SJ. DNA repair in *Mycobacterium tuberculosis*. What have we learnt from the genome sequence? *Mol Microbiol* 1998;29:1331-9.
4. Sassetti CM, Boyd DH, Rubin EJ. Genes required for mycobacterial growth defined by high density mutagenesis. *Mol Microbiol* 2003;48:77-84.
5. Szklarczyk D, Franceschini A, Kuhn M, et al. The STRING database in 2011: functional interaction networks of proteins, globally integrated and scored. *Nucleic Acids Res* 2011;39:D561-8.

\*WL Ling 凌威廉  
 \*JW Fang 方俊薇  
 VLJ Wang 王亮節  
 ASY Lau 劉錫賢  
 JCB Li 李振邦

# Effect of IL-17 in enhancing innate immunity to mycobacterial infection

## Key Messages

1. Interleukin (IL)-17A specifically enhanced mycobacteria-induced IL-6 production in human macrophages.
2. IL-17A together with tumour necrosis factor- $\alpha$  could modulate mycobacteria-induced immune responses.
3. The nitric oxide production induced by mycobacteria could be further upregulated by IL-17A.
4. IL-17A suppressed the survival of intracellular mycobacteria.

## Introduction

According to the World Health Organization, more than two billion people, equivalent to one third of the world's population are infected with *Mycobacterium tuberculosis* (MTB), and there are 12 million new cases and 1.5 to 2 million deaths attributable to this pathogen every year. Over the last decade, in Hong Kong, there have been about 6000 new cases every year. Although the incidence, prevalence, and mortality have declined gradually, eradication of the disease is difficult because of its long incubation time. The use of *M bovis* bacilli Calmette-Guerin (BCG) is effective in protecting against tuberculosis in newborns, but poorly effective in adults. The recent increase in the number of tuberculosis infections can be attributable to the AIDS epidemic and the emergence of multidrug-resistant strains. Development of more effective vaccination protocols and therapy for MTB is needed.

The bacilli causing active disease occurs in only a small proportion of the infected population because in most subjects the disease remains dormant and latent. Manifestation of the disease mainly depends on the immune status of the infected individual; the chance of manifestation of the disease is about 10% during a lifetime, and is presumed to ensue when the patient becomes immunocompromised.<sup>1</sup>

Macrophages are effector phagocytes involved in pathogen recognition and cytokine induction during immune response against mycobacteria. The interaction between macrophages and mycobacteria begins with the recognition of MTB or its components through different surface pattern recognition receptors on macrophages (eg toll-like receptors). This results in the upregulation of proinflammatory cytokines such as tumour necrosis factor (TNF)- $\alpha$ , interleukin (IL)-1 $\beta$ , IL-6, as well as free radicals such as nitric oxide (NO). The production of these cytokines effectively constrains the dissemination of mycobacterial infection.

IL-17 is a key proinflammatory cytokine produced by a specific group of T lymphocytes known as T-helper 17 (TH17) cells. The TH17 cells and the cytokines (IL-17 and IL-23) they secrete are associated with various human autoimmune diseases including rheumatoid arthritis, multiple sclerosis, and inflammatory bowel disease. Over-production of IL-17 in the tissues contributes to inflammation. Secretion of other proinflammatory cytokines (IL-1 $\beta$ , IL-6, and TNF- $\alpha$ ) can be stimulated by human macrophages. Through upregulation of proinflammatory mediators, IL-17A can mediate the infiltration of immune cells (neutrophils and monocytes) to the areas of inflammation.<sup>2</sup> We therefore examined the role of IL-17A during mycobacterial infection in macrophages, especially with respect to the dysregulation of cytokine and NO production and subsequent biological events.

## Methods

This study was conducted from December 2009 to November 2011. Recombinant human and mouse IL-17A was purchased from R & D Systems (Minneapolis, MN, USA). Antibodies against phospho-JNK, JNK, phospho-p38 MAPK, p38 MAPK, phospho-ERK1/2, and ERK were purchased from Cell Signaling

\* WL Ling and JW Fang contributed equally to this study

Hong Kong Med J 2013;19(Suppl 5):S15-8

LKS Faculty of Medicine, The University of Hong Kong:  
 Molecular Chinese Medicine Laboratory  
 WL Ling, JW Fang, VLJ Wang  
 Department of Paediatrics and Adolescent Medicine  
 ASY Lau, JCB Li

RFICID project number: 09080542

Principal applicant and corresponding author:  
 Dr. James Chun-bong Li  
 Molecular Chinese Medicine Laboratory,  
 LKS Faculty of Medicine, The University  
 of Hong Kong, Pokfulam Road, Hong Kong  
 SAR, China  
 Tel: (852) 28199863  
 Fax: (852) 28199863  
 Email: jamesli@hku.hk

Technology (Beverly, MA, USA). HRP-conjugated goat anti-rabbit antibody was purchased from BD Transduction Laboratories (San Diego, CA, USA). HRP-conjugated rabbit anti-goat antibody was purchased from Invitrogen (Carlsbad, CA, USA).

Murine macrophage cell line RAW264.7 was obtained from American Type Culture Collection (Rockville, MD, USA). Lyophilised *M bovis* BCG Danish strain 1331 was purchased from Statens Serum Institut (Copenhagen, Denmark). According to manufacturer's specification, the vaccine strain was free from contamination by MTB antigens. The lyophilised bacteria were freshly reconstituted with vaccine diluent before being added to the macrophages.

Human primary blood macrophages (PBMac) were isolated by centrifugation with the use of Ficoll-Paque PLUS (GE Healthcare, Piscataway, NJ, USA) and purified by a culture plate adherence method as described previously.<sup>3</sup>

Culture supernatants from treated macrophages were harvested, followed by centrifugation at 13 200 rpm for 5 minutes to remove cell debris. The culture supernatants were mixed with an equal volume of modified Griess reagent (Sigma-Aldrich, St Louis, MO, USA) and incubated in the dark for 10 minutes. Absorbance readings at 570 nm were taken, and the production of NO measured.

The intracellular bacteria in colony forming units were recovered based on methods described previously.<sup>4</sup>

Total RNA extraction using TRIZOL reagent (Invitrogen, Carlsbad, CA, USA), cDNA synthesised from reverse transcription using random hexamers (Amersham Biosciences, Piscataway, NJ, USA), SuperScript II RT (Invitrogen), and the details of RT-PCR were as described in our previous report.<sup>5</sup>

To perform Q-PCR, the levels of IL-6, IL mRNA, as well as reference gene (internal control) GAPDH and 18S RNA were assayed by the gene-specific Assays-on-Demand reagent kits (Applied Biosystems, USA). All samples were run in duplicate or triplicate and with no template controls on an ABI Prism 7700 Sequence Detector and Roche 480II.

MTT (3-(4,5-dimethylthiazol-2-yl)-2,5-diphenyltetrazolium bromide) assays were used to test cytotoxicity according to our previously described method.

## Results

### *IL-17A-enhanced mycobacteria-induced nitric oxide production*

During mycobacterial infection, the innate immune system produced different mediators including NO and cytokines to fight the pathogens. As human primary blood macrophage is not a producer of NO in vitro, a murine macrophage

cell line (RAW264.7) was used to investigate the effects of IL-17A on mycobacteria-induced NO production, and BCG was used to represent mycobacterial infection. This mycobacterial infection model has been showed to induce innate immune responses such as cytokine production and necrosis. We first assessed whether the BCG infection and the treatment of IL-17A could lead to excess cell death of RAW264.7 cells. We treated the cells with IL-17A (25 ng/mL) for 24 hours, followed by incubation with the BCG (multiplicity of infection [MOI]=1) for 8 to 48 hours, and measured the cell viability by MTT assay. The results demonstrated that the treatment with IL-17A and BCG did not induce cell death in RAW264.7 cells up to 72 hours of incubation. Therefore, our subsequent results were not due to the cell death response. We next examined whether IL-17 could enhance NO production by BCG. We treated RAW264.7 cells with IL-17 (25 ng/mL) for 24 hours, followed by incubation with BCG (MOI=1) for 32 or 48 hours. The concentration of NO in the supernatant was measured using the Griess reagent. The results demonstrated that BCG could induce NO production in RAW264.7 cells after incubation for 32 to 48 hours. In addition, IL-17 could enhance BCG-induced NO production. Therefore, IL-17A may act through this pathway to control the mycobacterial infection.

### *IL-17A specifically upregulated BCG-induced IL-6 production*

Apart from NO production, cytokine activation was also an important defence mechanism in the innate immunity to combat mycobacterial infection. Our previous reports indicated that BCG could induce cytokine production in PBMac, and therefore this model was used to study the role of IL-17A in BCG-induced cytokine responses. To investigate whether IL-17A differentially regulates BCG-induced IL-6, IL-10, TNF- $\alpha$ , and IL-1 $\beta$  expression, the kinetic profiles of both cytokines at mRNA and protein levels were measured by PCR/Q-PCR and ELISA, respectively. For IL-6, its mRNA expression showed enhanced expression following IL-17A pretreatment. The enhancing effect was observed at both short (4 hours) and long (24, 48, and 56 hours) time points, and the effect was most significant at 48 and 56 hours, with 14 and 7 times more than the fold induction by treatment with BCG pretreated with mock, respectively. In addition to mRNA level changes, ELISA results also showed corresponding increased IL-6 protein levels in a time-dependent manner, and the extent of increase was most obvious at 32 hours with 2.6-fold enhancement and the effect was most significant at 56 hours with a 2.3-fold increase. We also examined whether IL-17A could affect the expression levels of other proinflammatory cytokines including TNF- $\alpha$  and IL-1 $\beta$ . The PBMac were treated with IL-17A for 4 hours prior to the infection of BCG for additional 4, 8 and 24 hours. The RT-PCR results showed that BCG could induce both TNF- $\alpha$  and IL-1 $\beta$  mRNA expression in PBMac within 4 hours after infection. The pretreatment of IL-17A did not affect mRNA expression of TNF- $\alpha$  and IL-1 $\beta$ . In addition, we examined the expression

of the signature anti-inflammatory cytokine, IL-10 in IL-17A pretreated BCG-infected PBMac. The pretreatment with IL-17A could reduce the mRNA expression of IL-10. We further measured the protein level of IL-10 in the culture supernatant. However, the ELISA results showed that IL-17A had no significant effect on the level of IL-10 protein production.

In previous reports, BCG-induced IL-6 production could be via the activation of MAPK and PI3 kinase. Therefore, we examined the expression level of phosphorylated form of ERK1/2, p38 MAPK, and JNK. In order to examine the activation of kinases, PBMac were pretreated with 100 ng/mL of IL-17A or mock for 4 hours and then incubated with or without BCG (MOI=1) for the 30 and 60 minutes. Western blots revealed that IL-17A enhanced the phosphorylation of ERK1/2, but not p38 MAPK and PI3K. In addition to enhanced BCG-induced kinases activation, IL-17A increased mRNA stability of IL-6 to enhance its production. In previous reports, TNF- $\alpha$  was shown to enhance IL-6 mRNA stability in human myofibroblasts. Therefore, we examined whether IL-17A could interact with BCG-induced TNF- $\alpha$  to enhance IL-6 production. By treating the PBMac with neutralising antibodies to TNF- $\alpha$ , IL-17A-enhanced IL-6 production was abolished. In summary, our results demonstrated that IL-17A could specifically enhance mycobacteria-induced IL-6 production but not other proinflammatory and anti-inflammatory cytokines. This enhancement could be due to IL-17A-increased IL-6 mRNA stability and the interaction of IL-17A and TNF- $\alpha$ .

### ***IL-17A suppressed the intracellular survival of mycobacteria***

As IL-17A could enhance NO production and IL-6 expression in macrophages, we further examined whether IL-17A could affect the survival of mycobacteria in macrophages. PBMac were treated with 100 ng/mL of IL-17A for 24 hours, followed by infection with BCG for another 72 hours. After that, PBMac were lysed and the numbers of live BCG were measured by a colony forming unit assay. The results demonstrated that IL-17A could inhibit the intracellular survival of BCG in a dose-dependent manner. IL-17A could affect the innate immune responses against mycobacterial infection through the cytokine dysregulation and production of anti-mycobacterial products, and subsequently suppress mycobacteria survival.

### **Discussion**

IL-17A plays an important role in mediating the immune response during mycobacterial infection through the dysregulation of cytokines and free radicals. In cytokines dysregulation, IL-17A enhances the expression of IL-6, but not IL-10, IL-1 $\beta$ , and TNF- $\alpha$ . IL-6 is a proinflammatory cytokine that mediates inflammation and is essential for TH17 differentiation. Its enhanced production in PBMac by IL-17A suggests a positive feedback mechanism that favours

TH17 development and consequent IL-17A production. This is consistent to IFN- $\alpha$ -induced IL-12 production by macrophages during mycobacterial infection; both IFN- $\alpha$  and IL-12 are essential for Th1 cell development. Apart from regulating T-cell differentiation, IL-6 is also involved in host defence against mycobacterial infection through activating and maintaining effector functions of macrophages and T cells.

In addition to the direct mediation of transcription mechanisms, TNF- $\alpha$  also plays a crucial role in the IL-17A-enhanced IL-6 expression. The phenomenon of augmented IL-6 production may be due to the synergism between IL-17A and BCG. This synergistic effect on inflammatory protein expression implies that IL-17A and microbial components can cooperatively increase COX-2 levels. Moreover, co-treatment of IL-17A with other cytokines (TNF- $\alpha$ , IL-1 $\alpha$ , and IFN- $\alpha$ ) leads to an increase in IL-6 production. Although IL-17A did not upregulate TNF- $\alpha$  expression in our study, IL-17A could interact with the BCG-induced TNF- $\alpha$  to enhance the expression of IL-6.

In response to microbial infection, macrophages eliminate the phagocytosed pathogens by innate defence mechanisms. The bactericidal effect of NO towards intracellular mycobacteria has been noted in murine models. Our results showed that IL-17A could enhance NO production in the presence of mycobacterial infection. Nonetheless, IL-17A alone could not induce the NO production. The effects of IL-17A pretreatment on enhancing NO production may result from priming of innate immunity against mycobacterial infection.

### **Conclusions**

IL-17A may prepare the host immune system to respond quickly and effectively in fighting against mycobacterial infection. This finding may contribute to the development of new therapeutic agents against mycobacterial infections.

### **Acknowledgement**

This study was supported by the Research Fund for the Control of Infectious Diseases, Food and Health Bureau, Hong Kong SAR Government (#09080542),

### **References**

1. Young DB, Perkins MD, Duncan K, Barry CE 3rd. Confronting the scientific obstacles to global control of tuberculosis. *J Clin Invest* 2008;118:1255-65.
2. Kolls JK, Linden A. Interleukin-17 family members and inflammation. *Immunity* 2004;21:467-76.
3. Li JC, Au KY, Fang JW, et al. HIV-1 trans-activator protein dysregulates IFN- $\gamma$  signaling and contributes to the suppression of autophagy induction. *AIDS* 2011;25:15-25.
4. Yim HC, Li JC, Pong JC, Lau AS. A role for c-Myc in regulating anti-

- mycobacterial responses. *Proc Natl Acad Sci U S A* 2011;108:17749-54.
5. Fang JW, Li JC, Au KY, Yim HC, Lau AS. Interleukin-17A differentially modulates BCG induction of cytokine production in human blood macrophages. *J Leukoc Biol* 2011;90:333-41.

JCB Li 李振邦  
 LLY Chan 陳勵儀  
 HCH Yim 嚴志濠  
 BKW Cheung 張嘉華  
 DCW Lee 李振威  
 ASY Lau 劉錫賢

# Suppression of cellular antibacterial effects by HIV

## Introduction

In 2007, over 33 million people were HIV positive, of whom a large percentage progressed to fulminant AIDS. People infected with HIV gradually lose their immune system and become infected with other opportunistic pathogens. HIV infects and integrates its viral genome into CD4<sup>+</sup> T cells and macrophages. The viral proteins produced in infected cells dysregulate cellular responses, and in some cases lead to cell death. HIV transactivator protein (Tat) is one of the first viral proteins produced in infected cells. The primary function of Tat is to activate the HIV long terminal repeat (LTR) region, which contains the viral transcription activation sites, and to enhance the retroviral replication. With this Tat protein, HIV viral replication efficiency can be enhanced more than 100 fold. Tat can also dysregulate cytokine responses and affect AIDS pathogenesis.<sup>1-3</sup> It induces cytokines such as IL-10, IL-6, and TNF- $\alpha$  in monocytes/macrophages to activate HIV replication, induce T cell death, and promote HIV-associated B cell lymphomas.

As HIV can perturb and evade the host immune system, other pathogens take advantage of the immunocompromised state and invade the HIV-infected host. Co-infections with non-HIV pathogens including viruses, parasites, fungi, and bacteria are common in AIDS patients. These opportunistic infections change the course of disease progression, decrease host survival, and increase the risk of HIV transmission.

*Mycobacterium tuberculosis* (MTB) infection affects one third of the world's population and results in 1.5 to 2 million deaths annually. In Hong Kong, there are about 6000 new cases every year. According to the World Health Organization, countries with a high incidence of HIV infection also have higher incidence of tuberculosis. For hosts with normal immunity, only 10% of MTB-infected patients develop active disease. In the remaining 90%, the disease is latent. Latent MTB is reactivated when host immunity is perturbed such as in HIV infection, malnutrition, or after the use of immunosuppressive drugs.<sup>4</sup> The exact mechanism of tuberculosis reactivation remains unclear. Coinfection of HIV and MTB or *M avium* complex (MAC) is important in AIDS pathogenesis.

Gram-negative bacterial infections are also common in HIV-infected hosts. Lipopolysaccharide (LPS), the bacterial cell wall component of Gram-negative bacilli, is recognised by Toll-like receptor 4 and induces signalling cascades that trigger innate immune responses. Cytokines such as TNF- $\alpha$ , IL-6, and IFN- $\beta$  are produced to combat invading pathogens. For example, in mouse models, IFN- $\beta$  induces iNOS expression to enhance nitric oxide (NO) synthesis to help clear Gram-negative bacteria.<sup>4</sup> Furthermore, IFN- $\beta$  synergises with TNF- $\alpha$  and IL-1 $\beta$  to induce indoleamine-2,3-dioxygenase expression that inhibits bacterial growth.<sup>4</sup> In HIV-1 infected patients, induced cytokines may become dysregulated and contribute to the septic shock syndrome. This study aimed to elucidate the perturbation of cellular signalling pathways by HIV, specifically the Tat protein, to aid design of novel immunotherapeutic regimens to abrogate or lessen the severity of cytokine dysregulation.

## Methods

This study was conducted from February 2007 to January 2009. Recombinant

## Key Messages

1. Immunopathogenesis of HIV and mycobacterial infections is discussed.
2. HIV transactivator protein (Tat) is the viral factor responsible for favouring mycobacterial growth. This can be reversed by immunoregulatory cytokines such as IFN- $\gamma$ .
3. The use of small molecule inhibitors of Tat to abrogate its suppressive effects on the immune functions of macrophages/monocytes may have a role on the design of new therapeutic strategies against both pathogens.

*Hong Kong Med J* 2013;19(Suppl 5):S19-23

Department of Paediatrics and Adolescent Medicine, LKS Faculty of Medicine, The University of Hong Kong

JCB Li, LLY Chan, HCH Yim, BKW Cheung, DCW Lee, ASY Lau

RFCD project number: 06060612

Principal applicant:

Prof Allan Sik-yin Lau

1/F, New Clinical Building, Department of Paediatrics and Adolescent Medicine, The University of Hong Kong, Queen Mary Hospital, Hong Kong SAR, China

Corresponding author:

Dr. James Chun-bong Li

Molecular Chinese Medicine Laboratory, LKS Faculty of Medicine, The University of Hong Kong, Pokfulam Road, Hong Kong SAR, China

Tel: (852) 28199863

Fax: (852) 28199863

Email: jamesli@hku.hk

HIV-1 Tat protein was purchased from Advanced BioScience Laboratories (Kensington, MD, USA). Endotoxin levels of Tat protein was  $<0.0025$  EU/mg as measured by Pyrotell assay kit (Associates of Cape Cod, East Falmouth, MA, USA). The biological activities of the Tat protein were confirmed by HIV-LTR luciferase activities. Lipopolysaccharide extracted from *Escherichia Coli* serotype O26:B6 was purchased from Sigma-Aldrich (St Louis, MO, USA).

Primary blood monocytes (PBMo) were isolated from buffy-coat samples (donated by healthy volunteers), using the Ficoll-Paque (Pharmacia Biotech, Uppsala, Sweden) density gradient centrifugation. CD14<sup>+</sup> PBMo were purified from these cells using anti-CD14 magnetic beads (Miltenyi Biotec, Auburn, CA, USA). Cell viability was over 99% as measured by the Trypan blue exclusion assay, and the purity of monocytes was 90 to 95% as verified by FACS using PE-conjugated anti-CD14 antibody (Beckman Coulter, Miami, FL, USA). Purified CD14<sup>+</sup> PBMo were resuspended in RPMI containing 5% autologous plasma before culture. Primary human blood macrophages (PBMac) were obtained by an adherence method and cultured for 14 days in RPMI with autologous serum.

Total cellular RNA extraction and cDNA synthesis were performed as described in our previous reports.<sup>1-3</sup> The cDNA produced was then subjected to quantitative real-time polymerase chain reaction (QRT-PCR) assay using Applied Biosystems TaqMan probes including IFN- $\beta$ , GAPDH, and 18S rRNA (reference gene). Results of QRT-PCR were analysed with reference to the comparative C<sub>t</sub> (cycle number to threshold) according to the manufacturer's instructions. All samples were run in triplicate along with template controls.

The U133 Plus 2.0 Microarray is composed of >54 000 probe sets that can be used to analyse over 47 000 human transcripts and variants. Microarray procedures, including RNA quality control, sample labelling, gene chip hybridisation, and data acquisition, were undertaken together with the Genome Research Centre, University of Hong Kong. The quality of total RNA was checked by the Agilent 2100 Bioanalyzer. The RNA was then amplified and labelled with MessageAmp II-Biotin Enhanced Single Round aRNA Amplification Kit (Ambion, USA). Briefly, total RNA (1  $\mu$ g) was reverse transcribed to double-stranded cDNA by using an oligo(dT) primer bearing a T7 promoter. The double strand cDNA was then used as a template for in vitro transcription to generate biotin-labelled cRNA. After fragmentation, 15  $\mu$ g of cRNA was hybridised to the microarray gene chips for 16 hours. The gene chips were washed and stained using the GeneChip Fluidics Station 450 (Affymetrix, USA), and then scanned with the GeneChip Scanner 7G (Affymetrix, USA).

The IFN- $\beta$  bioassay was performed as previously described,<sup>3</sup> but with minor modifications. Supernatants from

the PBMac treated with different stimulants were collected. The collected samples or 400 pg/mL recombinant IFN- $\beta$  (PBL, Piscataway, NJ, USA) were mixed with control rabbit immunoglobulin fraction (Dako, Glostrup, Denmark) or rabbit anti-IFN- $\beta$  neutralising antibodies (Abcam, Cambridge, UK) and incubated for 30 minutes before being added onto T98G cells. After 24-hour incubation, the adherent T98G cells were washed with PBS and infected with encephalomyocarditis virus (EMCV) [ $10^8$  titre/mL] and cultured in 2% foetal bovine serum medium. After being infected for 24 hours, the virus-induced cytopathic effects were visualised using light microscopy after staining the cells with 0.1% crystal violet dissolved in 5% ethanol.

PBMac were fixed and stained with anti-NF $\kappa$ B p65 antibodies (Santa Cruz Biotechnology) followed by rhodamine-conjugated secondary antibodies (Millipore). Cell nuclei were stained with 4,6-diamidino-2-phenylindole dihydrochloride. Immunofluorescence of the stained cells was quantified by Cellomics ArrayScan HCS VTI Reader (Thermo Fisher Scientific, Waltham, MA, USA). The nuclear translocation of NF $\kappa$ B p65 was determined by Nuclear Translocation BioApplications from Cellomics and expressed as nucleus/cytoplasm intensity ratio. A higher intensity ratio indicated a higher level of nuclear localisation of NF $\kappa$ B p65. Representative images were captured using a 40x objective lens by immunofluorescence microscopy.

The BCG vaccine, Danish strain 1331, was purchased from Statens Serum Institut. The concentration of BCG (range, 0.5-5 cfu per cell) used in the experiments was optimised in our previous projects. The vaccine was free from virulent mycobacteria. Multiple stains of MAC including *M avium* and *M intracellulare* were provided by the Department of Microbiology, University of Hong Kong. The mycobacteria were cultured in Middlebrook 7H9 broth and quantified on 7H10 agar plates (BD Difco). For the colony forming unit (CFU) measurement, cells were lysed and the lysate were cultured for the presence MAC in Middlebrook 7H9 broth and quantified on 7H10 agar plates. The colonies formed by MAC were counted.

Fluorescein-labelled *E coli* was purchased from Molecular Probes Primary human macrophages. Different treatments were incubated with MAC or fluorescein-labelled *E coli* for 2 hours. The surface unbounded bacteria were washed with PBS. The cells were fixed and analysed by flow cytometry.

PBMac incubated with fluorescein-labelled microspheres and FITC-labelled *E coli* were fixed with 1% paraformaldehyde and analysed by a flow cytometer (Elite, Beckman Coulter, Fullerton, CA, USA).

The culture supernatants were collected for NO measurement by Griess reagent system (Sigma). The sample supernatants were mixed with Griess reagent and measured by a microplate reader. The viability of the cells

was measured using the 3-(4,5-dimethylthiazol-2-yl)-2,5-diphenyltetrazolium bromide assay, and the results from the Griess experiment were normalised.

## Results

### *Tat inhibits phagocytosis of E coli but not MAC in human macrophages*

HIV-1 Tat protein activates HIV LTR promoter, enhances HIV replication, and dysregulates the cytokine response.<sup>1-3</sup> We hypothesised that HIV-1 Tat could modulate macrophage functions to provide a favourable milieu for opportunistic microbial infections. Gram-negative bacteria and MAC infections are commonly encountered in HIV-1-infected and AIDS patients. In normal host immune response, macrophages engulf the bacteria and degrade them in a process called phagocytosis. We investigated whether HIV-1 Tat could affect the phagocytosis of the bacteria. The first step was to investigate whether HIV-1 Tat could mediate the cellular uptake of the fluorescein-labelled microspheres into macrophages. Fluorescein-labelled microspheres were incubated with primary peripheral human blood macrophages (PBMac) for 30 minutes after HIV-1 Tat pretreatment for 24 hours. HIV-1 Tat inhibited endocytosis of the fluorescein-labelled microspheres (Fig a).

We then measured the effects of HIV-1 Tat on phagocytosis of microbes in macrophages. PBMac were pretreated with HIV-1 Tat protein for 24 hours, followed by MAC infection for 2 hours. The cells were then washed by phosphate buffer saline and lysed. The lysate were plated on the agar plate for 14 days and the colonies formed were counted. The colonies formed in HIV-1 treated or mock-treated samples were similar, and that HIV-1 Tat did not affect the phagocytosis of MAC (Fig b).

We also examined whether HIV-1 Tat could affect the phagocytosis of *E coli* by PBMac. The treatment was similar to the study of phagocytosis of MAC, in which PBMac were treated by two different doses of HIV-1 Tat for 24 hours prior to the addition of FITC-labelled *E coli* for 1 hour. The cells were fixed and the FITC signals were measured by flow cytometry. HIV-1 Tat suppressed the FITC-labelled *E coli* phagocytosis by about 30% in PBMac (Fig c). In summary, HIV-1 Tat suppressed the endocytosis of the microspheres and phagocytosis of *E coli*, but had no effects on MAC.

### *Tat and MAC did not affect PI3Kinase pathways*

To examine the effects of HIV on PI3K pathways, PBMac were pretreated with or without Tat (100 or 200 ng/ml) for 24 hours before the addition of MAC (MOI=4 CFU/cell) for various time points. For shorter time points, MAC was added for 0.5, 1, and 2 hours. Protein samples were collected by lysing the cells using a relevant lysis buffer. For longer time points, protein samples were collected on day 1, 4, and 6 after MAC was taken up. This was followed by trypsinisation and washing with PBS twice. The levels

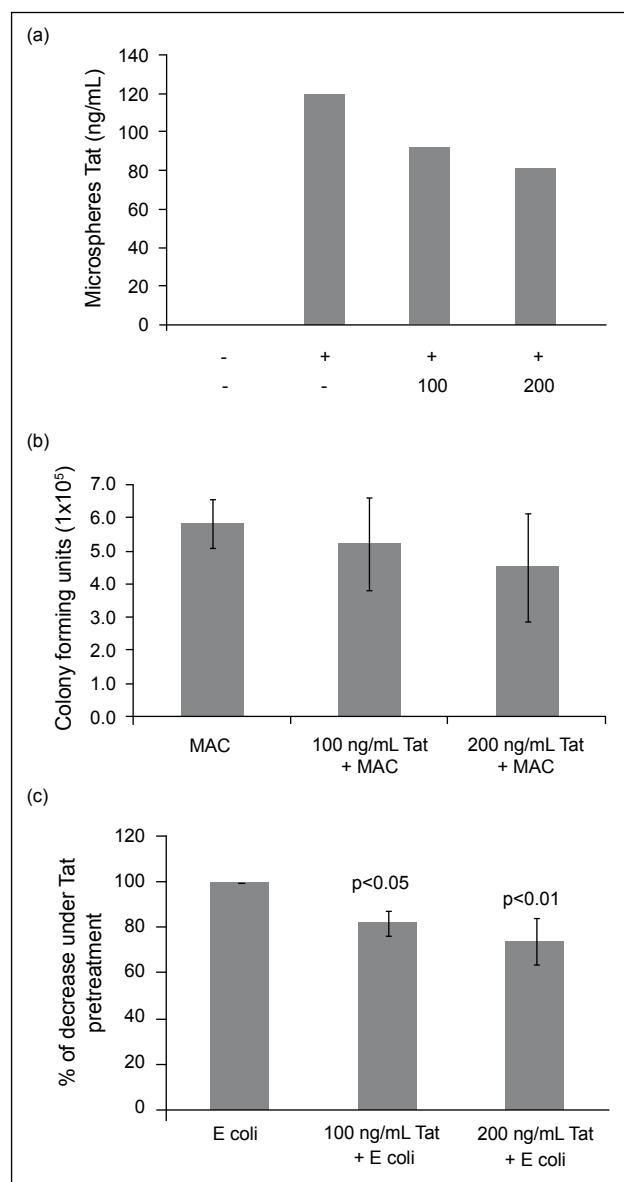


**Fig. (a) HIV transactivator protein (Tat) inhibited the endocytosis of fluorescein-labelled microspheres. (b) Tat did not affect the phagocytosis of *Mycobacterium avium* complex (MAC). (c) Tat inhibited the phagocytosis of *Escherichia coli*.**

of phospho-Akt (which is downstream of PI3Kinase) were measured by Western analysis. MAC did not activate the phosphorylation of Akt over the period of time points tested. Also, Tat did not affect MAC-induced phosphorylation of Akt at all time points tested.

### *Effects of Tat on iNOS pathways*

In previous reports, PBMac did not produce nitrite upon mycobacteria infection. Therefore, we used a mouse macrophage cell line RAW264.7, which is known to produce nitrite in vitro. Cells were pretreated with or without Tat (100 or 200 ng/ml) for 24 hours before the addition of BCG (MOI=1 CFU/cell) for 24 hours. Cell-free supernatants were collected and formation of nitrite was measured by the Griess assay. BCG induced nitrite formation in RAW cells

within 24 hours of treatment. However, Tat did not have any modulating effects on BCG-induced nitrite formation.

### **Microarray analysis**

To delineate the mechanisms underlying the effects of Tat on modulating immune responses during mycobacteria infection, we performed whole genome microarray experiments. Monocytes from five different individuals were treated with Tat. Total RNA from each sample was pooled together before performing the reverse transcription step. This was to contain the cost of genechip experiments and yet to provide a roadmap for QRT-PCR in each sample and also by Western blots for protein levels. Analyses of gene expression changes in Tat-treated cells (100 ng/ml for 3 hours) were compared to those cells with mock treatment alone. For analysis by the software GeneSpring GX, gene induction of greater than two fold was listed for confirmation by QRT-PCR. Tat upregulated the expression of phagocytosis-related genes including CD40 and CD44. These genechip analysis results formed the basis of our multiple projects.

### **Effects of mycobacteria on induction of phagocytosis-related genes**

As CD40 and CD44 could be upregulated by Tat, we further examined whether Tat could affect the CD40 and CD44 expression during mycobacteria infection. Human macrophages were infected with BCG (MOI=1 CFU/cell) for 0.5, 1, 3, and 6 hours. RNA samples were harvested and PCR of a panel of phagocytosis-related genes were performed. BCG did not increase any phagocytosis-related genes including CD14, CD32, CD35, and CD40 in human macrophages. The results also demonstrated Tat did not have additional effects on the expression of phagocytosis-related genes during mycobacterial infection.

### **Tat inhibits LPS-induced IFN- $\beta$**

As Tat could inhibit the phagocytosis of *E coli*, we further examined the cytokine expression profile of the blood monocytes/macrophages during Gram-negative bacterial infection in the presence of HIV-1 Tat. Lipopolysaccharide (from the outer membrane of the Gram-negative bacteria) contributes to the pathophysiological changes associated with sepsis. Its effects act through the dysregulation of cytokine (IL-6, TNF- $\alpha$ , and IFN- $\gamma$ ) production. We postulated that HIV-1 Tat may dysregulate the cytokine response to LPS and further cripple the immune system. PBMo were pre-incubated with HIV-1 Tat for 4 hours prior to LPS treatment for another 1 hour. As in previous studies, LPS induced IFN- $\gamma$  mRNA expression within 1-hour incubation. The IFN- $\gamma$  mRNA induction was inhibited in the presence of HIV-1 Tat protein in a dose-dependent manner (data not shown).

In order to delineate the mechanism of HIV-1 Tat on the suppression of LPS-induced IFN- $\gamma$  expression, we measured the activation status of transcription factor NF-kappa B, which plays a crucial role in IFN- $\gamma$  transcription.

Activation of transcription involves the translocation of an activated NF-kappa B p65 subunit from the cytoplasm to the nucleus for binding to the promoter of IFN- $\gamma$ . We measured the LPS-induced translocation of the NF-kappa B p65 subunit with or without the presence of HIV-1 Tat using an automated fluorescence screening system (Cellomics) and analysed the results using the computer programme (BioApplication). HIV-1 Tat abrogated the translocation of the LPS-induced NF-kappa B p65 subunit from the cytoplasm to the nucleus (data not shown).

As we delineated that HIV-1 Tat suppressed LPS-induced NF-kappa B activation and further inhibited IFN- $\gamma$  activation, we next investigated whether HIV-1 Tat could inhibit intracellular antiviral functions of macrophages. The antiviral activity of IFN- $\gamma$  was measured by its effects to protect the indicator cells (T98G, a human glioblastoma line) from EMCV-induced cytotoxicity. The presence of IFN- $\gamma$  inhibits EMCV from replicating in susceptible T98G cells. Supernatants from the PBMac treated with or without HIV-1 Tat and LPS were collected and transferred to the T98G cells. After 24-hour incubation of the T98G cells with the supernatants, EMCV were added to the cells for infection. LPS-treated supernatants protected the T98G cells from EMCV-induced cytotoxicity. With the HIV-1 Tat pretreatment of PBMac prior to LPS challenge, the protective effects were abrogated (data not shown).

In conclusion, HIV-1 Tat inhibits the LPS-induced cytokine response and further suppresses cellular antiviral activities. Such deficiency in antimicrobial responses may provide a favourable environment for HIV replication as well as for invasion by opportunistic pathogens, leading to progression of disease.

## **Discussion**

Both HIV-1 and mycobacteria have efficient immune evasion mechanisms to subvert immunity. IL-10 is induced by both infections through the double-stranded RNA dependent kinase and mitogen-activated kinases.<sup>1</sup> IL-10 is an anti-inflammatory cytokine capable of downregulating IL-2 synthesis and T-cell functions, and suppression of proinflammatory cytokine expression. Thus, both microbes and their encoded proteins are likely to act in concert to cripple cellular antimicrobial responses and enhance each other's survival and replication.

We have embarked a series of projects to explore the interactions between the two microbes at the cellular and molecular levels.<sup>1-3</sup> Results from this project are part of a larger effort to investigate the cross-talks and mechanisms. In the current study, HIV-1 Tat suppressed the endocytosis of the microspheres and phagocytosis of *E coli*, but had no effects on MAC. Both HIV Tat and MAC did not have effects on the activation of PI3K and the Akt system as reflected by respective phospho-protein kinase studies.

As Tat could inhibit the phagocytosis of *E coli*, we further examined the cytokine expression profile of the blood monocytes/macrophages during Gram-negative bacterial infection in the presence of HIV-1 Tat. HIV-1 Tat inhibits LPS-induced cytokine responses and further suppresses the cellular antiviral activities.<sup>3</sup> In other words, Tat cripples Toll-like Receptor-4 recognition of bacterial endotoxin, causing a deficiency in antimicrobial responses favourable to HIV replication.

High doses of Tat can induce the cytokine signalling suppressor gene SOCS-2 (one of a group of suppressors) to intervene with IFN- $\gamma$ -activated Jak-Stat1 signalling. This results in deficient MHC antigen II expression on the cell surface of antigen-presenting cells including fully differentiated primary human macrophages.<sup>2</sup> Thus, there is a tug of war between IFN-regulated activities against mycobacterial infection and the HIV-1-encoded Tat to subvert such cellular antimicrobial effects.

In conclusion, IFN- $\gamma$  may have a role in suppressing the action of HIV-1 in its enhancement of mycobacterial growth in human macrophages. This may provide a scientific rationale for the use of IFN- $\gamma$  and related cytokines in AIDS patients with aggressive mycobacterial infections. Alternatively, the use small molecule inhibitors of Tat to abrogate its suppressive effects on the immune functions of

macrophages/monocytes may have a role on the design of new therapeutic strategies against both pathogens.

### Acknowledgements

This study was supported by the Research Fund for the Control of Infectious Diseases, Food and Health Bureau, Hong Kong SAR Government (#06060612). We thank the Edward SK Hotung Paediatrics Education and Research Fund, the Hong Kong Society for Paediatric Immunology and Infectious Diseases and The University of Hong Kong for providing research awards. We also thank the International AIDS Society for granting permission to reproduce the figures.

### References

1. Li JC, Lee DC, Cheung BK, Lau AS. Mechanisms for HIV Tat upregulation of IL-10 and other cytokine expression: kinase signaling and PKR-mediated immune response. *FEBS Lett* 2005;579:3055-62.
2. Cheng SM, Li JC, Lin SS, et al. HIV-1 transactivator protein induction of suppressor of cytokine signaling-2 contributes to dysregulation of IFN- $\gamma$  signaling. *Blood* 2009;113:5192-201.
3. Yim HC, Li JC, Lau JS, Lau AS. HIV-1 Tat dysregulation of lipopolysaccharide-induced cytokine responses: microbial interactions in HIV infection. *AIDS* 2009;23:1473-84.
4. Flynn JL, Chan J. Immunology of tuberculosis. *Annu Rev Immunol* 2001;19:93-129.

Y Chen 陳揚超  
BC Wong 黃貝資  
CH Li 李其翰  
X Zhang 張小平  
SS Lee 李瑞山

# Triple combination lentiviral vector-based haematopoietic stem cell gene therapy for inhibition of drug-resistant HIV-1

## Key Messages

1. A triple combination lentiviral vector Lenti-TriC was successfully constructed, in which lhRNA targeting HIV-1 was driven by the U6 promoter, shRNA targeting CCR5 was driven by the H1 promoter, and TRIM5 $\alpha$  and EGFP were bicistronically expressed under the control of EF-1 $\alpha$  promoter.
2. Lenti-TriC expressed lhRNA (targeting HIV-1) and inhibited HIV-1 gene expression. Lenti-TriC expressed shRNA (targeting CCR5) and significantly inhibited CCR5 gene expression.
3. Lenti-TriC inhibited HIV-1 replication in human CEM T cells, primary PBMC cells, and macrophages.
4. Lenti-TriC did not affect the differentiation potential of CD34+ cells.
5. Lenti-TriC could be used for haematopoietic stem cell gene therapy to inhibit HIV-1 replication.

## Introduction

Although current combination therapies significantly decrease mortality, novel approaches are needed to prevent the emergence of resistant HIV-1 variants. RNA interference (RNAi) is a promising modality for inhibition of HIV-1 RNAs. The use of a single RNA (siRNA) or short hairpin RNA (shRNA) targeting viral and host proteins is reported to inhibit HIV-1 replication.<sup>1</sup> However, the use of siRNA or shRNA is limited owing to the emergence of RNAi-resistant escape viruses.<sup>2</sup> To avoid escape from RNAi, the virus should be simultaneously targeted by multiple shRNAs. Long hairpin RNAs (lhRNA) can be used to produce multiple effective siRNAs.<sup>3,4</sup>

Mammalian cells have developed diverse strategies to restrict retroviral infection. Tripartite motif-containing 5 isoform- $\alpha$  protein from rhesus monkey (TRIM5 $\alpha$ rh) restricts HIV-1 infection at a postentry, preintegration stage in the viral life cycle.<sup>5</sup> Stem cell-based gene therapy of HIV infection aims at inhibiting HIV replication and the progression to AIDS by the introduction of antiviral genes (eg siRNA) in primitive haematopoietic stem cells. To obtain sustained transgene expression and anti-viral protection in differentiated HIV-susceptible end-stage cells such as T cells and macrophages, CD34+ cells are widely used for gene transduction.<sup>1,5</sup> Lentivirus is an attractive vector for transducing CD34+ cells based on its high transduction efficiency and long-term expression of transgenes. We aimed to develop a triple combination lentiviral vector-based haematopoietic stem cell gene therapy for inhibition of HIV-1.

## Methods

This study was conducted from January 2009 to July 2011.

### Construction of a triple combination lentiviral vector

Lenti-TriC was constructed by multiple step cloning. For the construction of pU6-lhHIV, the U6 promoter, with a *Call* site at its 5'-end, was cloned into a pBluescriptKS(+) vector, bridging with lhHIV by a *Sall* site. The lhHIV sequence ended with an *EcoRI* site. For the construction of pH1-shCCR5, the H1 promoter, with a *Clal* site at its 5'-end, was cloned into a pBluescriptKS(+) vector, bridging with shCCR5 by a *Bgl* II site. The shCCR5 sequence ended with an *EcoRI* site. The EF-1 $\alpha$  promoter was linked at the 5'-end of chimeric TRIM5 $\alpha$  genes by Kozak sequence (5'-CGCTAGCGCTACCGGTCGCCACC-3'). The EF1 $\alpha$ -TRIM5 $\alpha$  was then cloned into pIRES2-EGFP by the 5'-*EcoRI* site and the 3'-*Sall* site. The EF1-TRIM5-IRES2-EGFP fragment was then obtained by restriction enzyme digestion at the *XbaI* and *EcoRI* sites.

The pU6-lhHIV was digested at *Clal* and *SmaI* sites to obtain the U6-lhHIV fragment. The pH1-shCCR5 was digested by *Clal*, and then blunted by polymerase, followed by digestion on the *EcoRI* site. The H1-lhCCR5 was released with the 5'-blunt end and the 3'-*EcoRI* site. The *SmaI* site of U6-lhHIV was ligated with the 5'-blunt end of H1-shCCR5 fragment, resulting in a U6-shHIV-H1-shCCR5 fragment with a 5'-*Clal* site and a 3'-*EcoRI* site. The U6-

*Hong Kong Med J* 2013;19(Suppl 5):S24-6

School of Biomedical Sciences, The Chinese University of Hong Kong

Y Chen, BC Wong, CH Li

Fu Med Biotech Bio-medicine Center, Shanghai Institutes for Biological Sciences, Chinese Academy of Sciences

X Zhang

Stanley Ho Centre for Emerging Infectious Diseases, The Chinese University of Hong Kong

SS Lee

RFID project number: 08070042

Principal applicant and corresponding author:

Dr Yangchao Chen

School of Biomedical Sciences, The Chinese University of Hong Kong, Shatin, NT, Hong Kong SAR, China

Tel: (852) 39431100

Fax: (852) 39431100

Email: frankch@cuhk.edu.hk

lhHIV-H1-shCCR5 fragment was cloned into the pSL6 vector at the ClaI and EcoRI sites.<sup>6</sup> The EF1 $\alpha$ -TRIM5 $\alpha$ -IRES2-EGFP fragment was cloned into the pSL6-U6-lhHIV-H1-shCCR5 fragment on its EcoRI and NheI sites, yielding the final product Lenti-TriC.

### **Lentivirus production and transduction**

The VSV-G-pseudotyped lentiviruses were produced by cotransfecting HEK293T cells with the transfer vector and three packaging vectors: pMDLg/pRRE, pRSV-REV, and pCMV-VSVG. Subsequent purification was performed using ultracentrifugation. For target cell transduction, 1000 cells were plated in 24-well plates and were transduced with lentivirus in the presence of 8  $\mu$ g/mL polybrene (Sigma). The culture medium was replaced after incubation for 12 hours. Transduced cells were sorted by means of fluorescence-activated cell sorting before use, when the transduction efficiency was less than 70% (based on enhanced GFP expression).

### **Isolation and culture of primary human cells**

Human peripheral blood mononuclear cells (PBMCs) were isolated by centrifugation in Ficoll-Hypaque (Sigma, St. Louis, MO, USA) from buffy coats of HIV-1-seronegative individuals. They were maintained in RPMI-1640 medium supplemented with 10% FBS in the presence of 2 mM L-glutamine, 1% Penstrep, and then stimulated with 5  $\mu$ g/mL phytohaemagglutinin (Sigma) and 200 U/mL interleukin-II (Invitrogen, USA) for 3 days before transduction with lentiviral vectors. Monocyte-derived macrophages were obtained from PBMCs by adherence to plastic for 12 hours in DMEM supplemented with 10% human serum (Cellgro, Herndon, VA, USA). They were then washed and cultured in the presence of macrophage colony-stimulating factor in 2 ng/mL DMEM (M-CSF, Sigma) for another 7 to 10 days, enabling the cells to fully differentiate before infection. The medium was replaced twice during the incubation period. The primary cells were maintained at 37°C with 5% CO<sub>2</sub> in a humidified incubator.

### **Generation of infectious HIV-1**

Infectious HIV-1 particles were generated using the proviral DNA construct pNL4-3 obtained from the National Institutes of Health AIDS Research and Reference Reagent Program. Two million HEK293T cells were transfected with 5 mg of proviral DNA using lipofectamine 2000 (Invitrogen). The virus titre was analysed for HIV-1 p24 antigen using an enzyme-linked immunosorbent assay (Beckman Coulter, Fullerton, CA, USA). The p24 values were calculated using a Dynatech MR5000 enzyme-linked immunosorbent assay plate reader (Dynatech Lab, Chantilly, VA, USA).

### **HIV-1 challenge and antiviral assays**

Cells were infected with vector or Lenti-TriC and then expanded for 72 hours. They were then challenged with recombinant HIV-1 NL4-3 virus at a multiplicity of infection of 0.01. After overnight incubation, the cells were washed three times with Hank's balanced salts solution and cultured

using the Roswell Park Memorial Institute's 1640 medium with 10% foetal bovine serum. At designated time points, culture supernatants were collected and analysed for HIV-1 p24 antigen using ELISA (Beckman Coulter, Fullerton, CA, USA). The p24 values were calculated.

## **Results**

### **Construction of a triple combination lentiviral vector**

We constructed a triple combination lentiviral vector (Lenti-TriC) targeting three stages of HIV-1 life cycle. Lenti-TriC contained a lhRNA targeting a conserved, untranslated region of HIV-1, the shRNA targeting CCR5, TRIM5 $\alpha$ , and EGFP cDNAs bicistronically under the control of the EF-1 $\alpha$  promoter (Fig 1).

We designed a 65 bp length hairpin RNAs targeting conserved HIV-1 untranslated 5' long terminal repeat for generating two effective shRNAs to inhibit HIV-1. This overcame the emergence of RNAi-resistant HIV-1, which is a frequent consequence after a single shRNA treatment. Lentiviral vector integrated into the host genome after transduction and enabled long-term expression of shRNAs and antiviral genes. Lentiviral vector could efficiently transduce CD34+ cells and offer the feasibility to transduce a large quantity of CD34+ cells for clinical application. Moreover, the anti-HIV effect mediated by CCR5 inhibition and overexpression of TRIM5 $\alpha$ rh was independent of the HIV RNA sequence, which was essential to obtain sustained anti-HIV efficacy, owing to the high mutation rate of the HIV-1 genome. Most importantly, the combination of lhRNA against HIV-1, shRNA targeting CCR5 and TRIM5 $\alpha$ rh cDNA into one single lentiviral construct inhibited HIV-1 at three different stages of its lifecycle: entry, postentry and preintegration, and replication.

### **Inhibition of HIV-1 replication in primary human PBMCs and macrophages**

To determine whether human PBMCs could be protected by the transduction of Lenti-TriC vectors, we isolated PBMCs from HIV-1-seronegative individuals, doubly transduced the PBMCs with lentiviral vectors, and then challenged the cells with HIV-1 NL4-3 virus. We observed a potent protective effect estimated to be a 9-fold reduction of p24 antigen levels in T cells transduced with Lenti-TriC at day 7 after challenging with HIV-1 NL4-3 virus (Fig 2). Notably, a positive protective effect was detected during almost the entire month of monitoring.

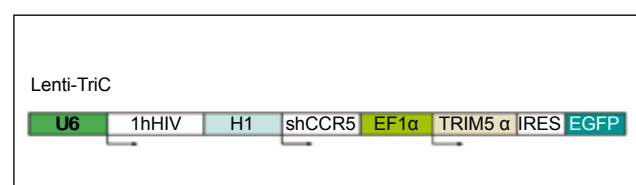


**Fig 1. Schematic diagram of Lenti-TriC**

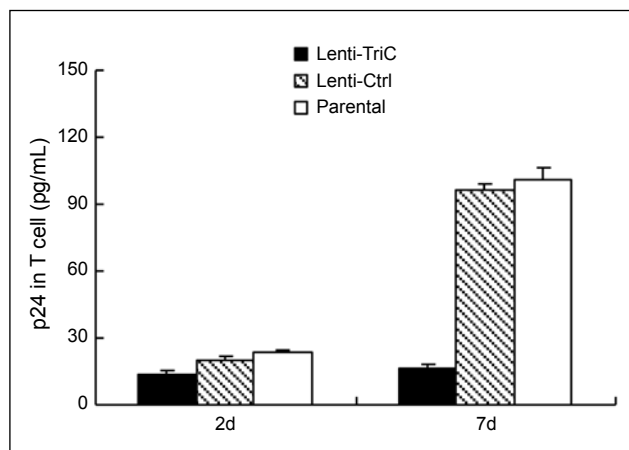


**Fig 2. Lenti-TriC inhibited HIV-1 replication in human primary peripheral blood mononuclear cells**

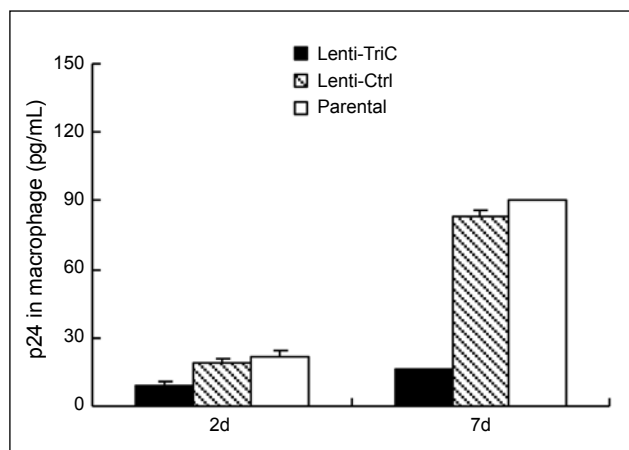


**Fig 3. Lenti-TriC inhibited HIV-1 replication in human primary macrophages**

To test the inhibitory effect on HIV-1 replication in human non-proliferating macrophages, these primary cells were transduced with the lentiviral vectors. These macrophages transduced with lentiviral vectors were then challenged with HIV-1 NL4-3 virus. During the 7 days of monitoring of these human macrophage challenge experiments, inhibition of HIV-1 replication was detected in the Lenti-TriC group (Fig 3). Notably, transduction efficiency with these SNV vectors for these primary human cells was approximately 30 to 40%.

## Discussion

Many gene therapeutic constructs with different mechanisms of action have been tested individually in both T-cell lines and haematopoietic stem cells. Owing to the complexity of the lifecycle and the high mutation rate of the HIV genome, the use of a single anti-HIV gene therapeutic construct is not adequate to afford extended viral protection.

We developed a triple combination lentiviral vector Lenti-TriC that targeted three stages of the lifecycle for the HIV gene in the haematopoietic stem cell setting. This lentiviral vector generated (1) lRNAs targeting a conserved untranslated region of HIV-1, (2) shRNAs targeting CCR5, and (3) expressed TRIM5 $\alpha$ . We tested the anti-HIV efficacy of Lenti-Tri-C in CEM T cells, human primary PBMCs, and macrophages. We also examined the usefulness of Lenti-Tri-C for HIV gene therapy by transducing CD34+ cells. Our results pave the way for the development of lentiviral vector-based hematopoietic stem cell gene therapy to inhibit HIV-1. However, all the data were based on in vitro cell culture studies; this was the limitation of this project. The main difficulty in carrying the experiments (and future animal/clinical studies) is to prepare sufficient amount of pure lentivirus.

## Acknowledgement

This study was supported by the Research Fund for the Control of Infectious Diseases, Food and Health Bureau, Hong Kong SAR Government (#08070042).

## References

1. Boden D, Pusch O, Ramratnam B. Overcoming HIV-1 resistance to RNA interference. *Front Biosci* 2007;12:3104-16.
2. Anderson J, Akkina R. CXCR4 and CCR5 shRNA transgenic CD34+ cell derived macrophages are functionally normal and resist HIV-1 infection. *Retrovirology* 2005;2:53.
3. Barichievy S, Saayman S, Von Eije KJ, Morris KV, Arbutnot P, Weinberg MS. The inhibitory efficacy of RNA POL III-expressed long hairpin RNAs targeted to untranslated regions of the HIV-1 5' long terminal repeat. *Oligonucleotides* 2007;17:419-31.
4. Sano M, Li H, Nakanishi M, Rossi JJ. Expression of long anti-HIV-1 hairpin RNAs for the generation of multiple siRNAs: advantages and limitations. *Mol Ther* 2008;16:170-7.
5. Anderson J, Akkina R. TRIM5 $\alpha$  expression restricts HIV-1 infection in lentiviral vector-transduced CD34+ cell-derived macrophages. *Mol Ther* 2005;12:687-96.
6. Chen Y, Lin MC, Yao H, et al. Lentivirus-mediated RNA interference targeting enhancer of zeste homolog 2 inhibits hepatocellular carcinoma growth through down-regulation of stathmin. *Hepatology* 2007;46:200-8.

JH Wong 王 灝  
 A Legowska  
 K Rolka  
 TB Ng 吳子斌  
 M Hui 許明媚  
 CH Cho 曹之憲  
 WW Lam 林蔚菱  
 SW Au 區詠娥  
 OW Gu 谷萬港  
 DC Wan 溫志昌

# Effect of human cathelicidin and fragments on HIV-1 enzymes

## Key Messages

1. Cathelicidins are small cationic antimicrobial peptides. Cathelicidin LL-37 and its fragments inhibit HIV replication. Whether there is any inhibitory effect on enzymes essential to the HIV life cycle is not known. Therefore, human cathelicidin LL-37 and its fragments were investigated for their ability to inhibit HIV reverse transcriptase, protease, and integrase.
2. Human cathelicidin LL-37 and its fragments LL13-37 and FK-16 inhibited HIV-1 reverse transcriptase dose-dependently, with respective  $IC_{50}$  values of 15, 7, and 70  $\mu$ M.
3. The three peptides inhibited HIV-1 protease with weak potency, achieving 20 to 30% inhibition at 100  $\mu$ M. The mechanism of inhibition was a protein-protein interaction as revealed by surface plasmon resonance.
4. The peptides did not inhibit translocation of HIV-1 integrase, labelled with green fluorescent protein, into the nucleus.
5. The peptides were not toxic to human peripheral blood mononuclear cells.

## Introduction

Multicellular organisms produce antimicrobial peptides for defence against microorganisms. One of these defence peptides is cathelicidin.<sup>1</sup> Cathelicidins are small cationic peptides widely distributed in tissues and bodily fluids, and were first found in bovine neutrophils.<sup>2</sup> They display antimicrobial anti-inflammatory and immunomodulatory activities.

Only an 18-kDa cathelicidin (hCAP18) is found in humans. Serine proteases catalyse the cleavage of hCAP18 to produce a cathelin domain and an antimicrobial peptide LL-37, which has diverse chemostatic activities towards monocytes, T cells, neutrophils, and mast cells. It stimulates interleukin-8 secretion, mast cell release of histamine, angiogenesis, and wound healing, while exerting no toxicity on lung epithelial cells when tested up to 111  $\mu$ M.

Novel therapeutic agents that prevent the transmission of HIV are needed. In mammals, defensins and cathelicidins are the two main types of antimicrobial peptides. Among cathelicidins, LL-37, protegrin-1, and indolicidin have anti-HIV activity. LL-37 is the only cathelicidin found in humans and can be cleaved in vivo into active fragments that are detected in human skin and sweat.

Human cathelicidin LL-37 and its fragments inhibit HIV-1 replication.<sup>3</sup> However, it is not known whether it and its fragments also inhibit enzymes essential to the life cycle of the HIV (HIV reverse transcriptase, HIV protease, and HIV integrase). We therefore investigated the human cathelicidin LL-37 and its fragments to determine their ability to inhibit HIV reverse transcriptase, protease, and integrase. Representative examples of at least three experiments are reported.

## Methods

This study was conducted from November 2009 to January 2011. LL-37 and its fragments LL13-37 and FK-16 were synthesised by the solid-phase method using Fmoc-chemistry. HIV reverse transcriptase activity was conducted using a commercially available ELISA kit (Boehringer).

For HIV integrase inhibitory activity, 24 hours before transfection, cultured HeLaTet-Off Advanced cells were seeded onto a culture dish in Dulbecco's modified Eagle's medium containing 10% foetal bovine serum. The EGFP-C-IN expression vector was transfected into HeLaTet-Off Advanced cells using Lipofectamine 2000 reagent. The medium was removed 5 hours after transfection. Fresh medium containing the test compound was added at a final concentration of 10  $\mu$ M DMSO was used as control. Twenty-four hours after transfection, cells were fixed with 4% paraformaldehyde in PBS for 15 minutes. Transfection results were analysed with a confocal microscope.

For HIV protease inhibitory activity, HIV-1 protease cDNA was cloned in pET3b, and transformed into *Escherichia coli* BL21(DE3)pLysS. HIV-1 protease expression was induced by IPTG. The expressed proteins (found predominantly as inclusion bodies) were analysed by SDS-PAGE. Bacterial

*Hong Kong Med J* 2013;19(Suppl 5):S27-30

The Chinese University of Hong Kong:

School of Biomedical Sciences

JH Wong, TB Ng, CH Cho, OW Gu, DC Wan

Department of Microbiology

M Hui

School of Life Sciences

WW Lam, SW Au

Department of Bioorganic Chemistry, Faculty

of Chemistry, University of Gdansk, Poland

A Legowska, K Rolka

RFCID project number: 09080402

Principal applicant and corresponding author:

Prof Tzi Bun Ng

Room 302B, Choh-Ming Li Basic Medical

Building, The Chinese University of Hong

Kong, Shatin, NT, Hong Kong SAR, China

Tel: (852) 2609 6872

Fax: (852) 2603 5123

Email: b021770@mailserv.cuhk.edu.hk

colonies which expressed a high level of 11 kDa HIV-1 protease were chosen for preparation of large-scale cultures. HIV-1 protease was purified from cultures. HIV-1 protease activity was assayed by cleavage of a fluorogenic substrate Arg-Glu(EDANS)-Ser-Gln-Asn-Tyr-Pro-Ile-Val-Gln-Lys(DABCYL)-Arg. After incubation at 37°C for 2 hours, the fluorescence intensity in each well was measured with an excitation wavelength at 340 nm and an emission wavelength at 490 nm.

A BIAcore 3000 surface plasmon resonance biosensor was used to measure the kinetic parameters of the interaction. Cathelicidin or its fragment (1nM) was covalently linked to the dextran on the surface of a CM5 sensor chip via primary amino groups using the Amine Coupling Kit (Pharmacia) at a flow rate of 5  $\mu\text{L}/\text{min}$ , 25°C. A range of 0 to 240 nM of HIV-1 reverse transcriptase in PBS was injected at a flow rate of 5  $\mu\text{L}/\text{min}$ , at 25°C, onto the cathelicidin or its fragments immobilised on the sensor chip surface. The binding surface was regenerated by 2M NaCl between sample injections. A control experiment was carried out similarly on an uncoupled sensor chip surface.

Human peripheral blood mononuclear cells (PBMCs) were isolated from the blood of healthy donors by density gradient using Ficoll-Paque Plus PBMCs ( $1 \times 10^5$ ) that were incubated with LL-37, LL 13-37, and FK-16 at 37°C for 24 hours. Then, a [3-[4,5-dimethylthiazol-2-yl]-2,5-diphenyltetrazolium bromide] solution was added and the plates were incubated for further 4 hours and then centrifuged. The supernatant was removed and dimethyl sulfoxide added to dissolve the formazan at the bottom of the wells. Ten minutes later, absorbance at 590 nm was determined.

## Results

After exposure for 24 hours at 37°C to various concentrations (0.98-125  $\mu\text{M}$ ) of LL-37, LL13-37, and FK-16, the viability of human PBMCs fluctuated from >80% to 100%, indicating minimal toxicity.

All three peptides exhibited a dose-dependent suppressive action on HIV-1 reverse transcriptase activity as disclosed by ELISA. The fragment LL13-37 was slightly more potent ( $\text{IC}_{50}=7 \mu\text{M}$ ) than LL-37 ( $\text{IC}_{50}=15 \mu\text{M}$ ). The fragment FK-16 was less potent ( $\text{IC}_{50}=70 \mu\text{M}$ ) than LL-37 and LL13-37.

The actions of the three peptides on HIV-1 protease are shown in Figure 1. The positive control pepstatin exerted a potent inhibitory action, achieving around 60% inhibition at a concentration of 10  $\mu\text{M}$ . In contrast, the inhibition elicited by LL-37 (about 22%), LL13-37 (about 30%), and FK-16 (about 30%), all at 100  $\mu\text{M}$ , was much less marked.

The positive control compound X (a proprietary ring compound isolated from a plant) was capable of inhibiting the translocation of HIV-1 integrase, labelled with green fluorescent protein, from the cytoplasm to the nucleus, because green fluorescence associated with the integrase was located outside the nucleus. The nucleus was stained red by propidium iodide. A merger showed the distinct separation of the red and green colours (data not shown).

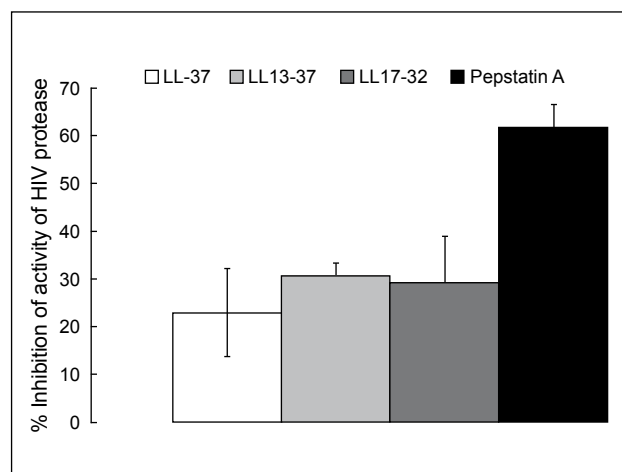


Fig 1. Inhibitory effect of human cathelicidin LL-37 (100  $\mu\text{M}$ ), and its fragments LL 13-37 (100  $\mu\text{M}$ ), 17-32 (100  $\mu\text{M}$ ), and positive control Pepstatin A (10  $\mu\text{M}$ ) on HIV-1 protease

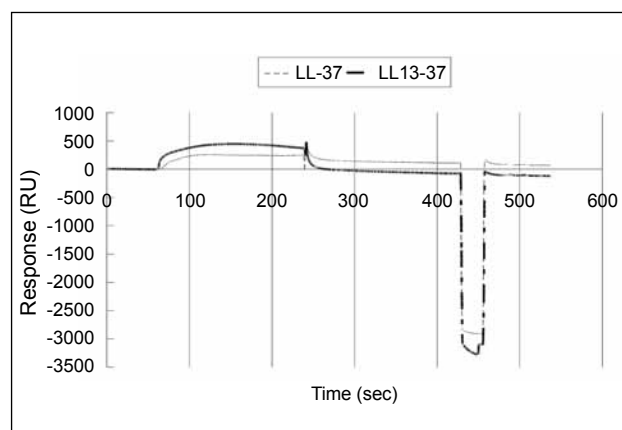


Fig 2. Assay of binding between HIV-1 protease (1  $\mu\text{M}$ ) and LL- 7/LL13- 7 (1  $\mu\text{M}$ ) using surface plasmon resonance (Biacore). 1  $\mu\text{g}$  was immobilised on the surface of a CM5 sensor chip. HIV-1 protease was injected at a flow rate of 5  $\mu\text{L}/\text{min}$ , starting at 60 seconds. The signals observed from 60 to 240 seconds represented protein-protein interaction between LL-37 and HIV-1 integrase. Washing with buffer from 240 to 420 seconds resulted in baseline response. Regeneration by washing with 2M NaCl resulted in a negative peak which appeared midway between 400 and 500 seconds. The results indicated protein-protein interaction between HIV-1 integrase and LL-37/LL13-37

After exposure to LL-37, LL13-37, and FK-16, all at 50  $\mu$ M concentration, the distribution of green fluorescence was similar to that in the control (data not shown). Green fluorescence revealing the location of HIV-1 integrase was detected in the nucleus, indicating that LL-37, LL13-37, and FK-16 lacked the ability to inhibit the translocation of HIV-1 integrase from the cytoplasm into the nucleus. Thus, it appears that among the three key HIV-1 enzymes, LL-37 and its fragments exhibited the most prominent inhibitory effects on HIV-1 reverse transcriptase; inhibition on HIV-1 protease was less marked while there was no inhibition of the translocation of HIV-1 integrase into the nucleus.

In the test of interaction between HIV-1 protease and LL-37/LL13-37 using surface plasmon resonance, the positive response recorded between 60 and 240 seconds indicated a protein-protein interaction between HIV-protease and LL-37/LL13-37 (Fig 2). Hence, this interaction contributed to the inhibitory effect of LL-37 and LL 13-37 on the activity of HIV-1 protease.

## Discussion

The antiviral activity of cathelicidins is well established. Human cathelicidin LL-37 and porcine cathelicidin protegrin-1 decrease lentiviral and retroviral vector infectivity. LL-37 lowers herpes simplex virus type 1 and adenovirus 19 titres. Corneal and conjunctival epithelial cells express LL-37 to protect against viral and bacterial ocular infections. LL-37 has been demonstrated to be virucidal and attacks the vaccinia viral envelop.

Cathelicidin is associated with HIV. Cervicovaginal secretions from Kenyan sex workers with sexually transmitted bacterial infections had heightened levels of LL-37, which were linked to escalated HIV acquisition.<sup>4</sup>

Human cathelicidin is expressed in human epididymal epithelium. It is detected in seminal plasma, and attached to sperm, indicating a role in fertilisation and in the antibacterial integrity of the male reproductive tract. Thus LL-37 may constitute a mechanism for post-coital protection against infection.

The ability to inhibit translocation of HIV-1 integrase from the cytoplasm to the nucleus has greater significance than inhibitory activity on the enzyme in view of the nuclear site of action of the enzyme. Neither cathelicidin LL-37 nor its fragments could inhibit integrase translocation. In the same assay a natural product, designated as compound X, was capable of impeding the process of integrase translocation.

LL-37 and its fragments produce the greatest inhibitory effect on HIV-1 reverse transcriptase. The peptides reduce the activity of HIV-1 protease but the potency of inhibition is low compared to that of the aspartyl protease inhibitor

pepstatin. The mechanisms of inhibition of HIV enzymes by homologous enzymes and natural products have been elucidated. HIV-1 protease lowers HIV-1 reverse transcriptase activity by the protein-protein interaction. Polysaccharopeptide from the medicinal mushroom *Coriolus versicolor* reduces the activity of HIV-1 reverse transcriptase by means of a mixed competitive and non-competitive mechanism.

Although the ranking of HIV-1 reverse transcriptase inhibitory activity is LL13-37>LL-37>FK-16, the ranking of HIV-1 protease inhibiting activity is LL13-37 $\approx$ FK-16>LL-37. LL13-37 is more potent than LL-37 in inhibiting HIV-1 reverse transcriptase and protease. It can be deduced that the first 12 N-terminal amino acid residues in LL-37 do not contribute to the inhibitory activity of LL-37 on the two HIV-1 enzymes. This is noteworthy, because LL13-37 is shorter and its chemical synthesis is easier. In contrast, LL13-32 displays a weaker HIV-1 reverse transcriptase inhibitory potency than LL-37 and higher HIV-1 protease inhibitory activity than LL-37. Thus, peptide fragments 14-16 and 33-36 have some contribution to the HIV-1 reverse transcriptase inhibitory activity of LL-37, but do not play a crucial role in its HIV-1 protease inhibitory activity. Thus, LL13-37 seems to be better than FK-16 in its potential applicability. It remains to be elucidated whether the same ranking of potency applies to the inhibitory effect of these cathelicidin peptides on HIV. The mechanism of inhibition of HIV-1 protease by LL-37 and LL13-37 has been demonstrated by surface plasmon resonance to be a protein-protein interaction. It is highly likely that an analogous mechanism of inhibition operates with regard to HIV-1 reverse transcriptase. None of the three cathelicidin peptides tested could inhibit nuclear translocation of HIV-1 integrase. The differential activity of cathelicidin peptides towards the three key HIV-1 enzymes is reminiscent of similar observations on some antifungal proteins and milk proteins.

## Acknowledgement

This study was supported by the Research Fund for the Control of Infectious Diseases, Food and Health Bureau, Hong Kong SAR Government (#09080402). Results of this study were published in: Wong JH, Legowska A, Rolka K, et al. Effects of cathelicidin and its fragments on three key enzymes of HIV-1. *Peptides* 2011;32:1117-22.

## References

1. Mendez-Samperio P. The human cathelicidin hCAP18/LL-37: a multifunctional peptide involved in mycobacterial infections. *Peptides* 2010;31:1791-8.
2. Zanetti M, Del Sal G, Storici P, Schneider C, Romeo D. The cDNA of the neutrophil antibiotic Bac5 predicts a pro-sequence homologous to a cysteine proteinase inhibitor that is common to other neutrophil antibiotics. *J Biol Chem* 1993;268:522-6.
3. Wang G, Watson KM, Buckheit RW Jr. Anti-human immunodeficiency virus type 1 activities of antimicrobial peptides derived from human and bovine cathelicidins. *Antimicrob Agents Chemother*

- 2008;52:3438-40.
4. Levinson P, Kaul R, Kimani J, et al. Levels of innate immune factors in genital fluids: association of alpha defensins and LL-37 with genital infections and increased HIV acquisition. *AIDS* 2009;23:309-17.

RWM Lung 龍偉明  
 JHM Tong 唐紅文  
 MYM Sung 宋影文  
 SL Chau 周淑玲  
 KW Lo 羅國煒  
 KF To 杜家輝

# Identification of Epstein-Barr virus microRNA in nasopharyngeal carcinoma cells

## Key Messages

1. The first small RNA library from Epstein-Barr virus (EBV) positive nasopharyngeal carcinoma (NPC) cells is constructed.
2. The large proportion of EBV-encoded microRNA (miRNA) compared to cellular miRNA in NPC cells underscores their significance in the establishment and/or maintenance of latent infections and pathogenesis in NPC cells.
3. The two newly identified EBV-encoded miRNAs, ebv-miR-BART-HK1 and ebv-miR-BART-HK2, are now published in [www.mirbase.org](http://www.mirbase.org) and named ebv-miR-BART22 (MIMAT0010132) and ebv-miR-BART21-5p (MIMAT0010130), respectively.

## Introduction

More than 600 human microRNAs (miRNA) have been identified as involved in numerous biological processes including cell proliferation, cell death, differentiation, morphogenesis, and development. After the discovery of Epstein-Barr virus (EBV)-encoded miRNAs in lymphoma cells, viral-encoded miRNAs become increasingly recognised in the role of carcinogenesis.

Nasopharyngeal carcinoma (NPC) is prevalent in Southern China (including Hong Kong) and is associated with EBV. Successful cloning of EBV miRNA from lymphoma cell lines demonstrates that EBV has the potential to exploit RNA silencing as a convenient mechanism for the regulation of host and viral gene expression. Current data on EBV miRNA are largely derived from EBV-positive lymphoma cell lines. Data on expression of EBV miRNAs in epithelial malignancy are scanty, as are comprehensive data on the expression profile of EBV-encoded miRNAs in NPC cell lines. To enhance understanding of NPC tumorigenesis and provide new diagnostic and therapeutic prospects, we investigated the EBV miRNA expression profile in NPC cells by construction of miRNA libraries from EBV-positive NPC cell lines and xenografts.

## Methods

This study was conducted from January 2007 to January 2008.

### *Cell lines, xenografts, and primary tumours*

For library construction, an EBV-positive NPC cell line (C666-1) and a xenograft (X2117) were used. To compare the expression of novel EBV-encoded miRNAs, a panel of EBV-positive cells including four lymphoid cell lines (Raji, Namalwas, BC-1, and Akata), four NPC xenografts (X666, X1915, C15, and C17), and EBV-negative immortalised normal nasopharyngeal epithelial cells (NP460 and NP69) were included. In all, 23 primary NPC biopsies were obtained from our Department of Anatomical and Cellular Pathology.

### *Cloning of miRNAs*

Enriched small-RNA fractions for library construction were collected with the miVana miRNA Isolation Kit (Ambion). Cloning miRNAs mainly followed the manufacturer's protocol for miRCat™ small RNA cloning kit (Integrated DNA Technologies, Coralville, IA, USA). In brief, the 3' and 5' cloning linkers were ligated to the small RNA, and cDNA was synthesised and amplified. After concatenation, the fragment was cloned and sequenced using the TOPO TA Cloning Kit (Invitrogen).

### *Bioinformatic analysis*

The extracted small RNA fragments  $\geq 18$  nt were annotated to the genome. The known human and EBV miRNAs were identified by blasting the sequences to miRBase. The remaining sequences were individually blasted to NCBI databases. Cloned sequences that matched the wild-type EBV genome (NC\_007605) were examined. The putative precursor sequence of 50 nt 5' and 3' of the clone sequences were extracted from the EBV genome for prediction of fold-back structure by MFOLD.

*Hong Kong Med J* 2013;19(Suppl 5):S31-5

Department of Anatomical and Cellular Pathology, Prince of Wales Hospital, The Chinese University of Hong Kong  
 RWM Lung, JHM Tong, MYM Sung, SL Chau, KW Lo, KF To

RFCID project number: 06060372

Principal applicant and corresponding author:  
 Prof Ka Fai To  
 Department of Anatomical and Cellular Pathology, Prince of Wales Hospital, The Chinese University of Hong Kong, Shatin, NT, Hong Kong SAR, China  
 Tel: (852) 26322361  
 Fax: (852) 26376274  
 Email: [kfto@cuhk.edu.hk](mailto:kfto@cuhk.edu.hk)

### Detection of miRNA expression by Northern Blot and real-time RT-PCR

For Northern Blot analysis, 10  $\mu$ g of total RNA were separated in 12% urea-PAGE, electroblotted onto Nytran Supercharge membrane (Schleicher & Schuell, Germany) and fixed by UV-crosslinking. Oligodeoxynucleotide probes were end-labelled with [ $\gamma$ - $^{32}$ P]-ATP and hybridised at 28°C to 32°C overnight. The membrane was then exposed on X-ray film after several washes. For miRNA quantification, SYBR green quantitative RT-PCR assay was used. RNA was polyadenylated and reverse transcribed. SYBR RT-PCR with the iScript Universal primer and miRNA-specific primers were performed in the ABI PRISM 7500 Fast Real-time PCR system (Applied Biosystems).

### Results

Two individual libraries were constructed from two NPC cell samples: C666-1 NPC cell line and X2117 NPC xenograft. Of 1813 clones in the C666-1 small RNA library, 615 (34%) sequences matched known EBV miRNAs and

277 (15%) matched known human miRNAs in miRBase. In addition to the known miRNAs and virus-encoded miRNAs, 811 (45%) clones were human sequences and 33 (2%) were EBV sequences that showed no matches to any known miRNAs. Most of the human sequence clones were rRNA and tRNA fragments, and the EBV sequence clones were fragments of EBV-encoded small RNAs (EBER1 and EBER2). The remaining 4% showed no matches to any known RNAs (Fig 1a).

A similar distribution was found in the X2117 small RNA library, with both EBV and human miRNAs enriched to 45% and 39%, respectively, out of 1115 clones (Fig 1b). The EBV-encoded miRNAs showed differences in cloning frequencies (Table). In these two libraries, the most abundantly cloned EBV-encoded miRNAs were EBV-miR-BART7 (109 hits), miR-BART9 (467 hits), and miR-BART10 (251 hits) [Table 1]. EBV-miR-BART2, 11, 12, 13, 14, 16, 17-5p, 18, 19 were of low abundance, whereas EBV-miR-BART1, 3, 4, 5, 6, 8, 17-3p showed moderate copy numbers in the libraries. Not all the reported EBV-

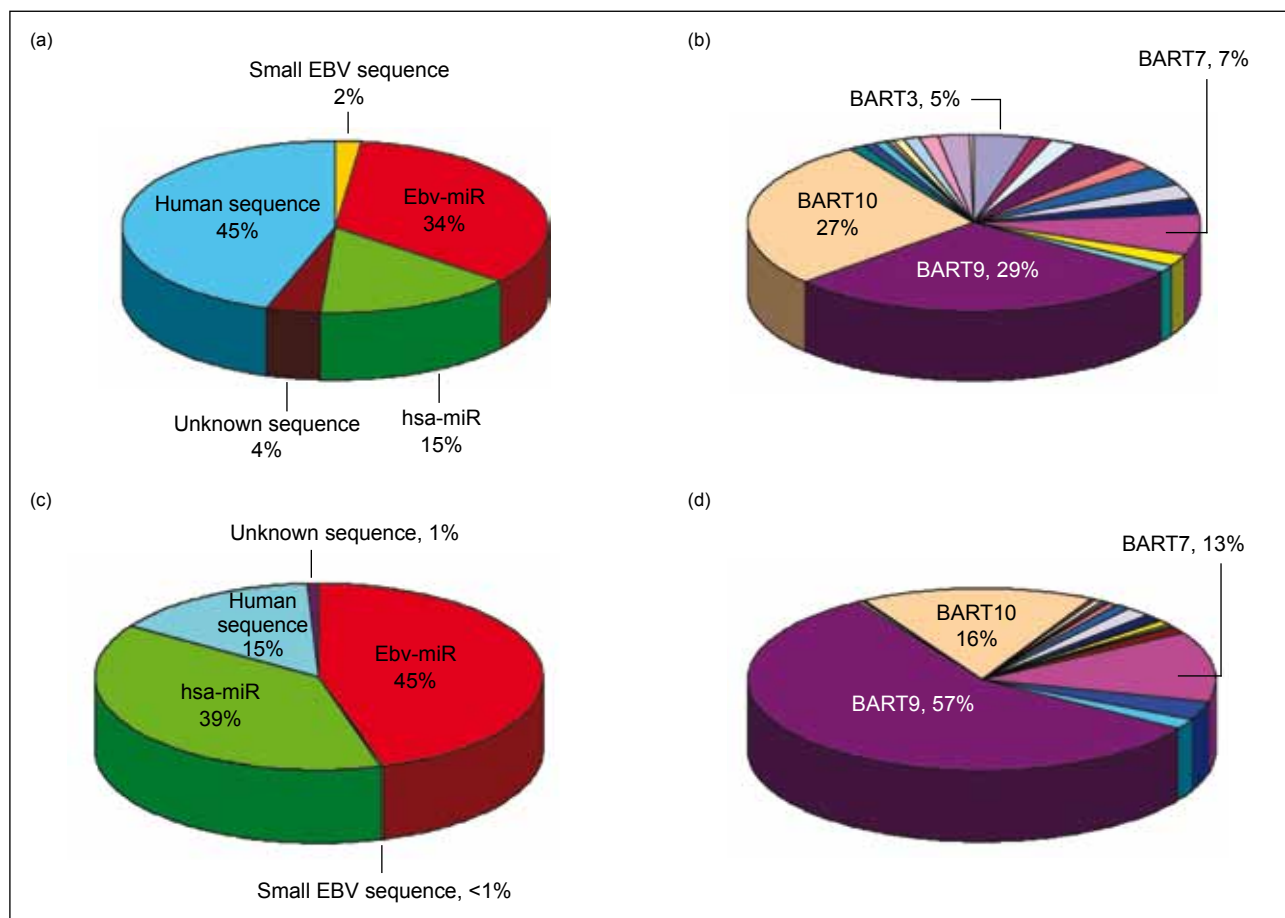


**Fig 1. Distribution of the small RNAs from libraries**

(a) A total of 1813 sequences were cloned from C666-1 cells. Among them, 34% corresponded to known Epstein-Barr virus (EBV) microRNAs (miRNAs) and 2% corresponded to the small EBV fragments. The distribution of the known EBV-miRNAs from C666-1 library (615 clones) was shown and the most frequently cloned miRNAs were listed. (b) A total of 1113 sequences were cloned from X2117. Among them, 45% corresponded to known EBV miRNAs and <1% was the other small EBV fragments. The distribution of the known EBV-miRNAs from X2117 library (500 clones) was shown and the frequently cloned miRNAs were listed

**Table. Cloning frequency of the known Epstein-Barr virus (EBV) microRNAs (miRNAs)**

EBV-miRNAs	No. of hits		Total
	C666-1 library	X2117 library	
BHRF1-1	0	0	0
BHRF1-2	0	0	0
BHRF1-3	0	0	0
BART1-5p	25	3	28
BART1-3p	9	2	11
BART2-5p	1	0	1
BART2-3p	0	0	0
BART3	30	6	36
BART3*	11	1	12
BART4	11	2	13
BART5	22	4	26
BART6-5p	18	0	18
BART6-3p	17	0	17
BART7	45	64	109
BART7*	0	0	0
BART8	15	16	31
BART8*	7	10	17
BART9	179	288	467
BART9*	0	0	0
BART10	169	82	251
BART10*	0	0	0
BART11-5p	7	0	7
BART11-3p	4	0	4
BART12	6	1	7
BART13	1	3	4
BART13*	0	1	1
BART14	5	0	5
BART14*	2	2	4
BART15	0	0	0
BART16	7	0	7
BART17-5p	9	0	9
BART17-3p	14	6	20
BART18-5p	1	0	1
BART18-3p	0	0	0
BART19-5p	0	1	1
BART19-3p	0	8	8
BART20-5p	0	0	0
BART20-3p	0	0	0
<b>Total</b>	<b>615</b>	<b>500</b>	<b>1115</b>

encoded miRNAs were present in our library. EBV-miR-BART2-3p, 7\*, 9\*, 10\*, 15, 18-3p, 20, and all the EBV-miR-BHRFs were not detected.

A small portion of EBV small RNA fragments that showed no matches to the known EBV-encoded miRNAs were identified from our libraries. They accounted for 1.2% (36 clones) of total reads. Sequence analysis of these clones identified two novel EBV-encoded miRNAs, which were temporarily designated as EBV-miR-BART-HK1 and EBV-miR-BART-HK2, respectively. The former was located between EBV-miR-BART9 and EBV-miR-BART10 in the EBV BART region. It has been cloned 20 times in C666-1 and once in X2117. In contrast, the latter was located upstream to BART cluster 2. It was cloned only once in the C666-1 library but not detected in X2117 library. Both miRNAs demonstrated stable hairpin structures with long paired stems by MFOLD.

By Northern blot analysis, both EBV-miR-BART-HKs were expressed in EBV-positive cell lines, xenografts and primary tumour samples, irrespective of their tissue origin (Fig 2). Expression of EBV-miR-BART-HK1 was greater in NPC cell lines, xenografts, and primary NPC samples than in lymphoid cell lines (Fig 2a). Expression of EBV-miR-BART-HK2 could also be detected in C666-1 and X2117, but the expression level was lower than EBV-miR-BART-HK1 in the same samples (Fig 2b).

We developed a more sensitive QRT-PCR assay for the detection of EBV-encoded miRNAs in biopsies. Using QRT-PCR, both novel EBV-encoded miRNAs were detected in all NPC biopsies and cell lines with relatively greater level of expression than in lymphoid cell lines. No

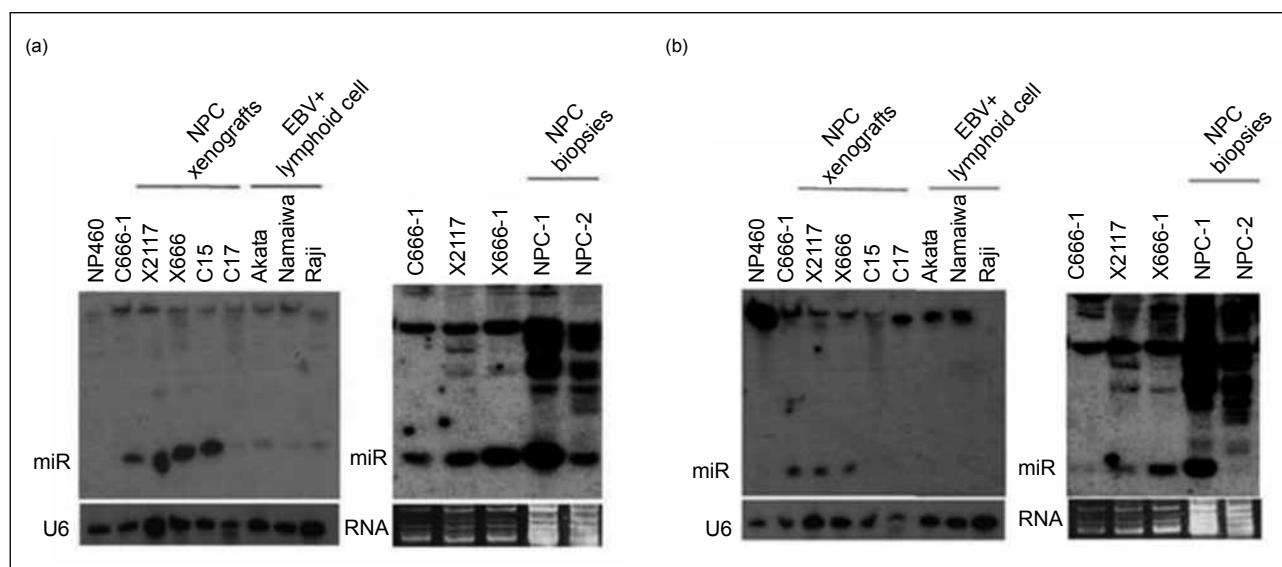


**Fig 2. Northern Blot analysis was performed for the expression of (a) Epstein-Barr virus (EBV)-miR-BART-HK1 and (b) EBV-miR-BART-HK2 on EBV-positive cells lines, two NPC xenografts (X2117 and X666), and two NPC biopsies. NP460 (control) was an EBV-negative normal nasopharyngeal epithelial cell line**

detectable EBV-miR-BART-HK1 or HK2 was found in the EBV-negative RNA samples. The results were consistent with the expression level as detected by Northern Blot.

## Discussion

The discovery of miRNAs as key players in the micromanagement of gene expression is a remarkable breakthrough in the field of molecular biology. In case of viral infection, the successful survival of viruses depends on their ability to exploit the biosynthetic machinery of host cells and inactivate the innate defence mechanisms of the host. It has been proposed that miRNAs are generated by viruses as a convenient mechanism to regulate host and viral gene expression. Therefore, they are the potential targets for gene therapies that are designed to block tumour development or progression.

Analysis of the miRNA sequences from our libraries indicated that EBV-encoded miRNAs accounted for over one third of the small RNA sequences detected in NPC cells. The large proportion of EBV-encoded miRNA (34% in the C666-1 library and 45% in the X2117 library) compared to cellular miRNA (45% in the C666-1 library and 39% in the X2117 library) underscored the significance of EBV-encoded miRNA in the establishment and/or maintenance of latent infections and the pathogenesis and malignant transformation in NPC cells. Greater expression of virus-encoded miRNA is common in transformed cell lines. For example, miRNA encoded by Marek's disease virus type 1 (MDV-1) and co-infected MDV-2 accounted for >60% of the 5099 sequences of the small RNA library from the MSB-1 cell.<sup>1</sup> miRNA-encoded by Kaposi's sarcoma-associated herpesvirus and EBV accounted for >40% of the entire miRNA pool from BC-1 cells.<sup>2</sup>

Not all the known EBV miRNAs were identified in our libraries (Table). We failed to clone any EBV-miR-BHRFs, as NPC cells were in EBV type II latency. The BHRF1 clusters of EBV miRNAs were selectively expressed in the lytic cycle and latency III cells, but not in cells undergoing type II or type I latency (such as NPC cells). In contrast, the viral BART miRNA cluster is highly expressed in NPC cells but barely detectable in lymphoid cells.<sup>2</sup> Northern analysis failed to detect EBV-miR-BHRFs in NPC cells (unpublished data). High-level expression of EBV miRNAs derived from the BART miRNA cluster was observed in the NPC cell line C666-1 and xenograft C15 without detectable expression of the miRNAs encoded within the BHRF1 cluster.<sup>2</sup>

Although the EBV BART miRNA cluster was highly expressed in NPC cells than in lymphoid cells, we failed to clone some of the miR-BARTs (eg EBV-miR-BART15 and EBV-miR-BART20) in our libraries. According to our previous report, miR-BART15 expression was not detected by Northern Blot in EBV-positive epithelial cells including C666-1 cell.<sup>3</sup> We also failed to detect several

minor strands of miRNA in the BART cluster (eg miR-BART7\*, miR-BART9\*, miR-BART10\*) despite the abundant expression of their major strands. During miRNA biogenesis, two strands of the miRNA duplex were derived. Normally only one of the dominant strands, the miRNA strand, was incorporated into the RNA-induced silencing complex and guided gene regulation. Although the non-miRNA was rapidly degraded, in many instances it was also captured during large scale cloning.<sup>1</sup> miR-BART7\*, miR-BART9\*, and miR-BART10\* were identified in low abundance from a large scale cloning study that generated more than 330 000 independent small RNA sequences from 256 small RNA libraries prepared from 26 distinct organ systems and cell types of humans and rodents.<sup>4</sup> Not surprisingly, we were not able to detect these minor strands in our library.

Annotation of the cloned RNAs revealed two novel EBV-encoded miRNAs. EBV-miR-BART-HK1 was located at a miRNA cluster within the intron of the BART gene, as previously reported for other miR-BARTs.<sup>2,5</sup> The expression of EBV-miR-BART-HK1 was greater in EBV-positive NPC cells than in lymphoma cell lines using Northern blotting. EBV-miR-BART-HK1 was located within the region deleted in the B95-8 EBV strain, thus explaining the lack of detection in a study in which EBV-encoded miRNAs were isolated from the human BL cell line BL41/95, which was infected with the EBV B95-8 strain.<sup>5</sup> This EBV strain has an approximately 12-kb deletion that removed a large part of the EBV BART gene. A relatively low level of expression of EBV-miR-BART-HK1 in lymphoma cells might be the reason for the lack of detection in another study in which EBV miRNAs were cloned from the lymphoma cell line BC-1.<sup>2</sup> Even in another large-scale cloning study, these two novel EBV-encoded miRNAs were also not detected.<sup>4</sup> The underlying explanation may require further investigation. The differential expression of EBV-miR-BART-HK1, like the BART mRNAs, may be preferentially expressed in EBV-infected epithelial cells and hence may play a particularly important role during EBV infection of this particular cell type. It will be interesting to study the biological function and target gene validation of the novel EBV miRNA EBV-miR-BART-HK1. Elucidating the contribution of EBV miRNAs to biological processes and disease will be crucial to exploit the emerging knowledge about miRNAs for the development of new human therapeutic application in EBV-related diseases.

## Conclusions

We are the first group to document the EBV-encoded miRNA expression in NPC cells and identified two novel EBV-encoded miRNAs. High levels of EBV-encoded miRNA expression compared to the cellular miRNA suggest that EBV-encoded miRNA might play a significant role in the establishment and maintenance of viral latency, and probably also in EBV pathogenesis and malignant transformation. Further studies are required to reveal

the functional significance of the novel miRNA in NPC biology.

### Acknowledgements

This study was supported by Research Fund for the Control of Infectious Diseases, Food and Health Bureau, Hong Kong SAR Government (#06060372). We also thank all the researchers for their hard work. Results of this study were published in part in: Lung RW, Tong JH, Sung YM et al. Modulation of LMP2A expression by a newly identified Epstein-Barr virus-encoded microRNA miR-BART22. *Neoplasia* 2009;11:1174-84.

### References

1. Yao Y, Zhao Y, Xu H, et al. Marek's disease virus type 2 (MDV-2)-encoded microRNAs show no sequence conservation with those encoded by MDV-1. *J Virol* 2007;81:7164-70.
2. Cai X, Schafer A, Lu S, et al. Epstein-Barr virus microRNAs are evolutionarily conserved and differentially expressed. *PLoS Pathog* 2006;2:e23.
3. Lo AK, To KF, Lo KW, et al. Modulation of LMP1 protein expression by EBV-encoded microRNAs. *Proc Natl Acad Sci U S A* 2007;104:16164-9.
4. Landgraf P, Rusu M, Sheridan R, et al. A mammalian microRNA expression atlas based on small RNA library sequencing. *Cell* 2007;129:1401-14.
5. Pfeffer S, Zavolan M, Grasser FA, et al. Identification of virus-encoded microRNAs. *Science* 2004;304:734-6.

RWM Lung 龍偉明  
 JHM Tong 唐紅文  
 MYM Sung 宋影文  
 PPS Leung 梁栢聲  
 SL Chau 周淑玲  
 DCH Ng 吳志恆  
 AWH Chan 陳永鴻  
 EKO Ng 吳啟安  
 KW Lo 羅國煒  
 KF To 杜家輝

# Identification and characterisation of Epstein-Barr virus miRNA in nasopharyngeal carcinoma cells

## Introduction

Nasopharyngeal carcinoma (NPC) is prevalent in Southern China, and clonal Epstein-Barr virus (EBV) genome has been detected in both high-grade dysplastic lesions and invasive carcinoma, implicating an important aetiological role for EBV in the NPC carcinogenesis. It is suggested that viral-encoded miRNAs play a significant role in carcinogenesis. We have identified novel EBV-encoded microRNAs from small cDNA library of native EBV-positive NPC cell line (C666-1) and xenograft (X2117) in our previous report (RFCID #06060372). These two miRNAs are highly expressed in NPC cell lines, xenografts, and primary tumour biopsies. In this study, we aimed to delineate the biological function of these novel EBV-encoded miRNAs in the nasopharyngeal epithelial cells.

## Methods

This study was conducted from January 2008 to December 2008.

### *Proliferation rate and cell-cycle analysis*

We studied the biological effect of miR-BART21 and 22 in two EBV-negative NPC cell lines (HK1 and HONE1) and an immortalised normal nasopharyngeal epithelial cell line NP69. Proliferation of cells transfected with miR-BART21 or 22 was assessed using the CellTiter 96 Non-Radioactive Cell Proliferation Assay (Promega, Madison, WI, USA). For flow cytometry analysis, cells were stained with propidium iodide and run on a FACScan flow cytometer (Becton Dickinson, CA, USA).

### *In vitro assay for Drosha complex digestion*

An in vitro Drosha processing assay was conducted to investigate the efficacy of miRNA biogenesis in different EBV strains. The digestion substrate was prepared by in vitro transcription from T7-added miR-BART22 PCR product (~300 nt) using MAXIscript kit (Ambion). The Drosha/DGCR8 enzymatic complex was purified by Flag Tagged Protein immunoprecipitation kit (Sigma, St Louis, USA) from 293FT cells transfected with Drosha and Flag-DGCR8 expression vectors and was mixed with 100 ng RNA substrate at 37°C for 1.5 hours. Digested products were analysed by Northern blot analysis.

### *In silico target prediction*

We used MiRanda prediction by adjusting the energy threshold to -15 kcal/mol and the cut-off score to 90. We used the default setting for RNAhybrid program prediction. The LMP2A reference sequence for target prediction was extracted from NCBI (AB290724).

### *Luciferase reporter assay*

293FT cells ( $1 \times 10^5$ ) grown in 24-well plates were co-transfected with miRNA and reporter construct for analysis. The cells were harvested after 2 days for luciferase activity analysis using Dual Luciferase Reporter Kit (Promega).

### *Western blotting and immunohistochemistry*

Western Blot was performed as previously described. The primary antibodies used were: LMP2A (MCA2467, AbD SeroTec; 1:2000 dilution), EGFP

## Key Messages

- Two novel Epstein-Barr virus (EBV) miRNAs (miR-BART21 and miR-BART22) are preferentially expressed in nasopharyngeal carcinoma (NPC) samples.
- Sequence polymorphisms in the primary transcript of miR-BART22 augment its biogenesis in vitro, and thus may underline the high and consistent expression of miR-BART22 in NPC cells.
- EBV latent membrane protein 2A (LMP2A) is a putative target of miR-BART22. It is postulated that modulation of LMP2A expression by miR-BART22 may permit escape of EBV-infected cells from host immune surveillance. The large proportion of EBV-encoded miRNA compared to cellular miRNA in NPC cells underscores their significance in the establishment and/or maintenance of latent infections and pathogenesis in NPC cells.

*Hong Kong Med J* 2013;19(Suppl 5):S36-8

Department of Anatomical and Cellular Pathology, Prince of Wales Hospital, The Chinese University of Hong Kong

RWM Lung, JHM Tong, MYM Sung, PPS Leung, SL Chau, DCH Ng, AWH Chan, KW Lo, KF To

Department of Surgery, The University of Hong Kong  
 EKO Ng

RFCID project number: 07060242

Principal applicant and corresponding author:  
 Prof Ka Fai To  
 Department of Anatomical and Cellular Pathology, Prince of Wales Hospital, The Chinese University of Hong Kong, Shatin, NT, Hong Kong SAR, China  
 Tel: (852) 2632 2361  
 Fax: (852) 2637 6274  
 Email: kfto@cuhk.edu.hk

(Clontech; 1:20,000 dilution) and  $\beta$ -actin (Sigma; 1:30,000 dilution). Immunohistochemical study was carried out using anti-LMP2A antibody (15F9, AbD SeroTec; 1:50) on the Ventana Nex ES automated stainer (Ventana Corporation, Tucson, AZ) using the avidin-biotin detection method.

## Results

### *Preferentially expressed miR-BART21 and miR-BART22 in NPC cells*

Greater expression of miR-BART21 and miR-BART22 was observed in NPC samples than in lymphoid cell lines (Akata, Namalwa, and Raji) using Northern blot and QRT-PCR analysis. Detailed comparison of the flanking sequences of miR-BART21 and miR-BART22 from C666-1 (EU828629.1) and Raji (AJ507799.2) revealed two nucleotide variations in miR-BART21 and four nucleotide changes in miR-BART22 (data not shown). The predicted secondary structures on miR-BART21 primary transcript (~300 nucleotides) [pri-miR-BART21] from Raji-EBV and C666-EBV strains were highly similar. However, the predicted secondary structure of miR-BART22 from Raji-EBV differed significantly from C666-EBV. The four nucleotide polymorphisms on Raji-EBV resulted in a small side-branched stem-loop adjacent to the mature miR-BART22 sequence (data not shown), which could impair miRNA maturation by concealing the DGCR8 recognition site in pri-miRNA processing. Although all four nucleotide variations in BART22 were positioned distal to the hairpin structure, changes to the two nucleotides (147144 A>T and 147146 C>A) could readily affect the stem-loop formation (data not shown). More importantly, 147144 A>T and 147146 C>A were identified in all 17 local NPC specimens examined. To elucidate whether nucleotide polymorphism of pri-miR-BART22 affected miRNA maturation, we examined the digestion efficiency of the Drosha/DGCR8 enzymatic complex by incubating immunoprecipitated flag-tagged Drosha/DGCR8 with in vitro transcribed EBV RNA substrates (AJ507799.2; 147137-147456) from the C666-1 and Namalwa EBV genomes, which shared the same polymorphism as Raji-EBV. In vitro digestion of pri-miR-BART22 in C666-1 was much facilitated in Drosha/DGCR8 processing, compared to the Namalwa strain (data not shown). Therefore, we hypothesised that nucleotide polymorphisms within the primary miR-BART22 transcript could augment its maturation in NPC cells, and at least partly explain the varying transcript levels in different EBV strains.

### *Functional effect of miR-BART21 and miR-BART22*

The functional effect of miR-BART21 and miR-BART22 on cell proliferation and the cell cycle was investigated in three EBV-negative cell lines (NP69, HK1, and HONE1). In all three cell lines, transfection of miR-BART21 or miR-BART22 precursor did not show morphologic changes as in mock experiments; nor did they alter the proliferation and cell cycle.

### *LMP2A is a potential target of miR-BART22*

In silico prediction suggested that LMP2A might be a putative target of miR-BART22. Using the luciferase reporter assay, we demonstrated that miR-BART22 exerted a strong inhibitory effect on LMP2A-3'UTR (42%,  $P < 0.001$ ). The repression was eliminated when the complementarities of the seed region were either deleted or mutated (data not shown). This suggests that the repressive property of BART22 on LMP2A 3'UTR was both functional and specific.

To confirm the importance of seed sequence complementarity in the BART22-LMP2A interaction, we performed additional luciferase assays using LMP2A-M1-M3 reporter plasmids with miR-BART22 and two miRNA mimics (miR-M2-BART22 and miR-M3-BART22) designed to compensate for the mutated seed regions of the LMP2A-M2 and M3 reporters (data not shown). The miRNA mimics exerted differing levels of suppression with the BART22 3'UTR, indicating that the miRNA mimics were functionally active. However in co-transfection with LMP2A-WT 3'UTR reporter, only miR-BART22 was able to suppress translation. Although seed binding may be critical for initiating repression, mutant miR-M3-BART22 with restored complementarity to LMP2A-M3 failed to exert an inhibitory effect on its corresponding mutated reporter. While miR-M2-BART22 significantly inhibited translation of the LMP2A-M2 mutated reporter, it expressed only slightly below the control level and clearly did not exhibit profound repression (data not shown). This suggests that the seed interaction between miR-BART22 and LMP2A-3'UTR was unique. Replacing seed pairing with other complementary sequences yielded negligible or only partial suppressive effects.

### *Differential expression of LMP2A in NPC cells*

To investigate whether LMP2A is commonly expressed in NPC cells, we performed both RT-PCR and Western blot on a panel of NPC samples from South China. Although LMP2A RNA transcript could be detected in C666-1 cells, and NPC xenografts X666 and X2117, none of them showed detectable LMP2A protein level in Western blot (data not shown). Nevertheless, we were able to detect weak focally expressed LMP2A in X2117 by immunohistochemical staining. In addition, we detected weak LMP2A expression in six out of 26 (23%) primary NPC tumours (data not shown). The expression levels of miR-BART22 and LMP2A mRNA were also determined in 11 of these tumours. Interestingly, the LMP2A mRNA expression level did not correlate directly with protein expression. This finding supports the possible regulatory role of miR-BART22 on LMP2A expression.

### *Suppression of LMP2A protein expression by miR-BART22*

To establish the strong interaction between miR-BART22 and LMP2A-3'UTR, two supportive experiments were designed. First, the dose effect of miR-BART22 on

LMP2A expression was studied by co-transfection of different amounts of miR-BART22 with the LMP2A expression vector with the complete 3'UTR. MiR-BART22 suppressed the LMP2A protein level in a dose-dependent manner without an apparent effect on LMP2A mRNA level (data not shown). MiR-BART22 expressions also had no obvious effect on the EGFP control protein. Second, transfection of miR-BART22 into HEK293 that had been stably transfected with pcDNA3.1-LMP2A (data not shown) readily suppressed the LMP2A protein. The transfection again had no significant effect on the LMP2A mRNA level. These results strongly suggest that LMP2A is a direct target of miR-BART22, which specifically represses LMP2A expression at the post-transcriptional level.

## Discussion

Transcriptional regulation of LMP2A in EBV-infected cells by epigenetic and viral latent protein mechanisms has been reported. In the current study, LMP2A could also be regulated at the translational level by miR-BART22. LMP2A protein was expressed in NPC biopsies, which tended to have relatively low expressions of miR-BART22. However, not all biopsies showing low miR-BART22 expression had detectable LMP2A. This indicates that LMP2A expression might also be regulated by other pathways. Such multiple regulatory mechanisms have also been implicated in LMP1 modulation.<sup>1</sup>

There are many potential benefits when LMP2A expression is suppressed during NPC development. LMP2A in particular has a stronger immunogenicity than two other EBV latent gene products (EBNA1 and LMP1). In this regard, limiting LMP2A protein expression has potential advantages for NPC cells to escape host immune surveillance, and thus LMP2A expression in NPC cells is predictably low. In fact, immunomodulatory effects of other EBV-miRNAs have recently been demonstrated. For example, down-regulation of LMP1 by miR-BARTs may favour immune escape by decreasing the antigen processing function of NPC cells.<sup>1</sup> In primary effusion lymphoma, EBV-miR-BHRF1-3 can target CXCL-11/I-TAC, an IFN-inducible T-cell attracting chemokines.<sup>2</sup> Apart from immunogenicity, LMP2A (as oppose to LMP1) could

suppress NF- $\kappa$ B level resulting in an anti-proliferative effect.<sup>3</sup> Moreover, LMP2A expressing epithelial cells could also inhibit telomerase reverse transcriptase activity, an enzyme important for cell immortalisation and transformation.<sup>4</sup> Since LMP2A has diverse functional roles in epithelial cells, its expression is therefore needed to be tightly regulated during the development of NPC.

We have reported that miR-BARTs regulates LMP1 expression,<sup>1</sup> and miR-BART5 affects the expression of the cellular target gene PUMA.<sup>5</sup> In this study, we further identified miR-BART22 as a modulator of an important oncogenic and immunogenic viral gene—LMP2A. This provides evidence for the vital roles of EBV-encoded miRNAs in regulating oncogenic and immunogenic latent viral protein expression, which may be important for the progression and survival of EBV-infected NPC cells.

## Acknowledgements

This study was supported by the Research Fund for the Control of Infectious Diseases, Food and Health Bureau, Hong Kong SAR Government (#07060242). We also thank all the researchers for their hard work. Results of this study were published in part in: Lung RW, Tong JH, Sung YM et al. Modulation of LMP2A expression by a newly identified Epstein-Barr virus-encoded microRNA miR-BART22. *Neoplasia* 2009;11:1174-84.

## References

1. Lo AK, To KF, Lo KW, et al. Modulation of LMP1 protein expression by EBV-encoded microRNAs. *Proc Natl Acad Sci U S A* 2007;104:16164-9.
2. Xia T, O'Hara A, Araujo I, et al. EBV microRNAs in primary lymphomas and targeting of CXCL-11 by ebv-mir-BHRF1-3. *Cancer Res* 2008;68:1436-42.
3. Stewart S, Dawson CW, Takada K, et al. Epstein-Barr virus-encoded LMP2A regulates viral and cellular gene expression by modulation of the NF-kappaB transcription factor pathway. *Proc Natl Acad Sci U S A* 2004;101:15730-5.
4. Chen F, Liu C, Lindvall C, Xu D, Ernberg I. Epstein-Barr virus latent membrane 2A (LMP2A) down-regulates telomerase reverse transcriptase (hTERT) in epithelial cell lines. *Int J Cancer* 2005;113:284-9.
5. Choy EY, Siu KL, Kok KH, et al. An Epstein-Barr virus-encoded microRNA targets PUMA to promote host cell survival. *J Exp Med* 2008;205:2551-60.

J Yu 于 君  
HC Jin 金洪傳

# Latent-lytic switch of Epstein-Barr virus infection in gastric carcinoma

## Key Messages

1. Epstein-Barr virus (EBV) causes gastric cancer and was almost always latent in infected tumour cells. Tumour cells infected with the latent stage of EBV do not respond to the antiviral drug ganciclovir. Zinc finger E-box binding factor (ZEB1) is the transcriptional repressor pivotal for silencing the BZLF1 promoter (Zp). BZLF1 is sufficient to convert EBV from the latent to lytic form. However, the mechanism of ZEB1 regulating latent-lytic switch of the EBV life cycle in EBV-associated gastric cancer and the virus's role in gastric carcinogenesis remain unknown.
2. We investigated the effect of ZEB1 on latent-lytic switch of EBV infection in gastric cancer cell lines. Loss or gain of ZEB1 biological function indicated its potential as a novel molecular target for the intervention in EBV-associated gastric cancer.
3. In addition, TaqMan real-time PCR was performed to examine the existence of EBV in primary gastric cancer and premalignant lesions. The association between EBV and patient characteristics was assessed.
4. Our results suggest that ZEB1 is a key mediator of the latent-lytic switch of EBV-associated gastric cancer. Inhibition of ZEB1 may be a potential means of therapy.

## Introduction

Epstein-Barr virus (EBV) is an infective agent causing gastric cancer.<sup>1</sup> It is almost always latent in infected tumour cells. Tumour cells infected with the latent form of virus do not respond to the antiviral drug ganciclovir (GCV). The intermediate-early gene BZLF1 is a transcriptional activator of viral genes essential for lytic replication.<sup>2</sup> Zinc finger E-box binding factor (ZEB1) is the transcriptional repressor pivotal for the silencing of the BZLF1 promoter (Zp),<sup>3</sup> indicating that the aberrant regulation of ZEB1 expression in tumour cells may have an important influence on EBV dormancy and persistence. However, the mechanism by which ZEB1 regulates the latent-lytic switch of the EBV life cycle in EBV-associated gastric cancer and its role in gastric carcinogenesis in the Chinese remain unknown. In this study, we evaluated the effect of ZEB1 in modulating the latent-lytic switch of EBV infection in gastric cancer cells, and the potential of ZEB1 as a novel molecular target for the intervention in EBV-associated gastric cancer. We also addressed the clinical importance of EBV infection in gastric carcinogenesis in a large-scale cohort of Chinese patients.

## Methods

This study was conducted from November 2008 to October 2010. Loss or gain of ZEB1 function was obtained by ZEB1 siRNA knockdown and ZEB1 overexpression in EBV-infected gastric cancer cell lines. Cell growth was evaluated by cell viability and a colony formation assay. The cell cycle distribution was determined by flow cytometry. The activity of Zp was examined after ZEB1 overexpression in AGS-EBV cells using a luciferase reporter activity assay.

Gastric cancer tissues were obtained from 711 primary gastric cancer patients in the First Affiliated Hospital of Sun Yat-sen University, Guangzhou from January 1999 to December 2006. In addition, 97 gastric tissues with precancerous lesions (intestinal metaplasia and/or atrophic gastritis) and 24 normal gastric tissues were collected. All patients and controls gave consent for participation, and the study protocol was approved by the Clinical Research Ethics Committee of the Sun Yat-sen University of Medical Sciences.

Genomic DNA was extracted from gastric tissue and EBV was detected using quantitative PCR and in situ hybridisation. ZEB1 expression level was examined by immunohistochemistry.

## Results

Knockdown of ZEB1 markedly enhanced expression of the lytic gene BZLF1 in YCC10 cells, compared to cells treated with the control siRNA. A well-known marker for latent EBV infection, EBNA1 expression was significantly inhibited by ZEB1 knockdown. ZEB1 knockdown caused about 20% inhibition in cell numbers, compared to control siRNA transfected YCC10 cells ( $P < 0.01$ ). Fluorescence-activated cell sorting (FACS) analysis revealed a significant decrease in the number of cells in the S phase in YCC10 cells with ZEB1 knockdown compared to control cells ( $P < 0.01$ ). In addition to this inhibition of cell proliferation, there was a significant increase in the number of cells accumulating in the G2/M phase following ZEB1 knockdown with YCC10 cells

*Hong Kong Med J* 2013;19(Suppl 5):S39-42

Institute of Digestive Disease, Prince of Wales Hospital, The Chinese University of Hong Kong

J Yu, HC Jin

RFICID project number: 08070522

Principal applicant and corresponding author:  
Dr Jun Yu

Room 707, Li Ka Shing Medical Sciences Building, Prince of Wales Hospital, Shatin, NT, Hong Kong SAR, China

Tel: (852) 3763 6099

Fax: (852) 2144 5330

Email: junyu@cuhk.edu.hk

( $P < 0.01$ ). We examined whether ZEB1 depletion could increase the sensitivity of gastric cancer cells to GCV. Following ZEB1 knockdown, GCV treatment demonstrated a significantly more additive effect on cell growth with 55% inhibition in cell viability ( $P < 0.001$ ), compared with YCC10 transfected with ZEB1-siRNA alone. Cellular apoptotic rate was determined using annexin-V-FITC/propidium iodide double staining. The number of early apoptotic cells 72 hours following ZEB1-siRNA transfection was substantially increased, as compared to control-siRNA transfected cells ( $P < 0.05$ ). Induction of apoptosis was further confirmed by analysis of two crucial apoptosis-related mediators of caspase-3 and PARP by Western blot. Enhanced expression of active forms of caspase-3 and PARP were demonstrated in YCC10 cells treated with ZEB1-siRNA. These results suggested that apoptosis concomitant with G2/M cell cycle arrest induced by down-regulation of ZEB1 was a plausible cause leading to the growth inhibition in ZEB1-depleted gastric cancer cells.

Overexpression of ZEB1 led to a significant inhibition of the EBV lytic gene (BZLF1) expression in AGS-EBV cells. The activity of Zp after ZEB1 overexpression in AGS-EBV cells was examined using the luciferase reporter activity assay. Our results indicated that the activity of Zp was significantly inhibited by ZEB1 re-expression ( $P < 0.001$ ). This suggests that ZEB1 inhibited BZLF1 transcription through reducing the activity of the BZLF1 promoter Zp. Ectopic expression of ZEB1 in AGS-EBV cells caused a significant increase of viable cells ( $P < 0.01$ ). The colony formation assay also confirmed that the colonies formed in ZEB1-transfected cells were significantly greater in number and larger in size than in empty vector-transfected cells (up to 100% of vector control,  $P < 0.001$ ). Moreover, FACS analysis of ZEB1-transfected AGS-EBV

cells revealed a significant induction in the number of S-phase cells compared to vector-transfected cells ( $P < 0.01$ ). Overexpression of ZEB1 downregulated protein expression of cleaved caspase-3, cleaved caspase-9, and cleaved-PARP compared with vector-transfected AGS-EBV cells, indicating reduced cell apoptosis.

The presence of EBV in gastric tissue specimens was determined with two EBV DNA fragments targeting the BamHI-W region and EBNA-1 regions. Using both the BamHI-W PCR and the EBNA-1 PCR, EBV DNA was detected in 80 (11.3%) of 711 gastric cancers, 4 (4.1%) of 97 precancerous lesions, but none from tissues of the 24 healthy controls. The proportion of EBV DNA-positive cases among these groups was significantly different ( $\chi^2 = 7.57$ ,  $P < 0.05$ ). EBV DNA-positive cases were significantly more frequent in patients with gastric cancer than in those with precancerous lesions ( $\chi^2 = 4.66$ ,  $P < 0.05$ ).

The association between clinicopathologic features and EBV infection in human gastric cancers is listed in the Table. The presence of EBV was associated with age ( $P < 0.05$ ), male gender ( $P = 0.0002$ ), intestinal histological type ( $P = 0.05$ ), and marginally associated with well or moderate differentiated gastric cancer ( $P = 0.08$ ). However, there was no correlation between the EBV and the tumour location, *Helicobacter pylori* infection, and survival of gastric cancer patients.

We evaluated ZEB1 expression in EBV-positive and EBV-negative primary gastric cancer tissues by immunohistochemistry. ZEB1 was more frequently detected in EBV-positive gastric cancers (80%, 12/15) than in EBV-negative gastric cancers (10%, 5/50) ( $P < 0.0001$ ).

**Table. Clinicopathologic features of gastric cancer patients with presence of Epstein-Barr virus (EBV)**

Variable	No. (%) of patients		P value
	EBV-positive (n=68)	EBV-negative (n=487)	
Mean±SD age (years)	53.66±13.08	57.00±12.60	
Gender			0.0002
Male	60 (15.9)	318 (84.1)	
Female	8 (4.5)	169 (95.5)	
Location			>0.05
Proximal	16 (11.1)	127 (88.9)	
Distal	45 (11.9)	333 (88.1)	
Lauren histologic subtype			0.05
Intestinal	60 (13.9)	371 (86.1)	
Diffuse	8 (6.7)	111 (93.3)	
Differentiation			0.0845
Poor	51 (14.6)	298 (85.4)	
Well or moderate	10 (8.1)	113 (91.9)	
Tumour node metastasis stage			0.6398
I	7 (9.6)	66 (90.4)	
II	6 (8.5)	65 (91.6)	
III	22 (11.5)	170 (88.5)	
IV	26 (14.0)	160 (86.0)	
<i>Helicobacter pylori</i> infection			0.110
Positive	18 (15.8)	96 (84.2)	
Negative	16 (8.4)	175 (91.6)	

## Discussion

Downregulation of ZEB1 in YCC10 causes upregulation of BZLF1 expression and downregulation of latent gene EBNA1 expression, thus promoting the latent-lytic switch of EBV infection. BZLF1 regulates the switch from latent infection to virus replication in EBV-infected cells and thus acts as a key mediator of reactivation from latency to the viral productive infection of EBV.<sup>4</sup> Expression of the BZLF1 gene is necessary and sufficient to disrupt EBV latency. EBNA1 is essential for maintenance of viral latent replication and persistence.<sup>5</sup> Thus, loss of ZEB1 may lead to reactivation into lytic replication due to the enhanced expression of BZLF1 and reduced expression of EBNA1. To better define the effect of ZEB1 in latent-lytic switch in gastric cancer, we examined its functional consequences by knocking down in the human gastric cancer cell line, YCC10. Decreased ZEB1 expression in YCC10 led to the inhibition of cell growth and S-phase cells, induction of apoptosis and caused cell cycle arrest in the G2/M phase. Induction of apoptosis was further confirmed by increased expression of activated form of caspase-3 and PARP, which leading to impairment of DNA repair and apoptosis. Thus, heightened ZEB1 depletion may diminish EBV-positive gastric cancer cell growth by upregulating apoptotic cell death pathways. Collectively, knocking down ZEB1 by itself was sufficient to induce EBV lytic replication in latently infected gastric cancer cell. We found that GCV alone was barely effective in controlling the YCC10, whereas induction of lytic EBV infection in YCC10 induced by re-expression of an immediate-early gene BZLF1 through knocking down ZEB1 enabled killing of the cells by GCV, because the host cells were in the lytic stage rather than the latent stage. EBV infection expressed virally encoded kinases to phosphorylate the prodrug GCV and changed to its cytotoxic form. As EBV-positive tumour cells are primarily in the latent form of EBV infection, induction of the latent-to-lytic switch of the EBV life cycle by ZEB1 inhibition could improve the clinical efficacy of GCV by specifically killing EBV-positive tumour cells and represents a new therapeutic option for EBV-associated gastric cancer.

We further investigated the role of the ZEB1 as a transcriptional repressor of BZLF1 and thus regulating the latent-to-lytic switch of the EBV life cycle in gastric cancer through again-of-function assay. Ectopic overexpression of ZEB1 in AGS-EBV led to downregulation of BZLF1. We further showed that this suppressive effect of ZEB1 on BZLF1 expression was specifically mediated through binding to a specific site of the BZLF1 promoter (Zp). This was supported by recent reports that ZEB1 can directly bind Zp via the ZV element, repressing transcription of BZLF1 initiated from Zp and therefore contribute to regulation of the switch between latency and lytic replication of EBV.<sup>3</sup> In addition, ectopic expression of ZEB1 in AGS-EBV cells showed a marked promoting effect on cell growth and cell proliferation. Moreover,

ectopic expression of ZEB1 in AGS-EBV cells reduced expression of pro-apoptotic genes including cleaved caspase-3, caspase-9, and PARP. These results inferred that over-expression of ZEB1 is sufficient to inhibit lytic reactivation by inhibiting transcription of BZLF1, and that ZEB1 indeed plays a central role in maintenance of EBV latency in gastric cancer cells.

The association between EBV infection and gastric cancer has not been well documented in Chinese. Existence of EBV in gastric cancer tissues was determined by two real-time quantitative PCR tests targeting different part of the EBV genome, BamHI-W and EBNA-1, respectively, and validated by EBER assay. In our cohort, we observed that EBV-positive gastric cancer comprises 11.3% (80/711) of cases. This is similar with the EBV prevalence detected in gastric cancer in other countries. The EBV-carrying tumours are observed more often in males ( $P < 0.001$ ) and in younger patients ( $P < 0.05$ ) [Table]. The trends toward male predominance and younger age have been observed in Japanese and Dutch gastric cancer patients. EBV infection was also detected in precancerous lesions (atrophy and intestinal metaplasia), although its frequency was distinctly lower in these lesions than in the tumours ( $P < 0.05$ ). The infection was not detected in normal gastric tissues. This indicated that EBV enters the gastric epithelium at an early stage of the multistep process of gastric carcinogenesis. This is in line with observations that EBV is the precursor lesion in precancerous and carcinoma cells. Thus, it is likely that EBV might infect a dysplastic gastric epithelial cell, transforming it into a carcinoma cell as an additional mechanism contributing to gastric malignant progression. ZEB1 was more frequently detected in EBV-positive gastric cancers than in EBV-negative gastric cancers ( $P < 0.0001$ ), consistent with ZEB1 being essential for maintenance of EBV latent replication and persistence in gastric cancer. In addition, the overall survival of the EBV-carrying gastric cancer patients showed no difference to those with the EBV-negative tumour. These results suggest that EBV plays a distinct role in gastric carcinogenesis in Chinese patients.

## Acknowledgement

This study was supported by the Research Fund for the Control of Infectious Diseases, Food and Health Bureau, Hong Kong SAR Government (#08070522).

## References

1. Fukayama M, Hino R, Uozaki H. Epstein-Barr virus and gastric carcinoma: virus-host interactions leading to carcinoma. *Cancer Sci* 2008;99:1726-33.
2. Le Roux F, Sergeant A, Corbo L. Epstein-Barr virus (EBV) EB1/Zta protein provided in trans and competent for the activation of productive cycle genes does not activate the BZLF1 gene in the EBV genome. *J Gen Virol* 1996;77:501-9.
3. Feng WH, Kraus RJ, Dickerson SJ, et al. ZEB1 and c-Jun levels contribute to the establishment of highly lytic Epstein-Barr virus infection in gastric AGS cells. *J Virol* 2007;81:10113-22.

4. Speck SH, Chatila T, Flemington E. Reactivation of Epstein-Barr virus: regulation and function of the BZLF1 gene. *Trends Microbiol* 1997;5:399-405.
5. Humme S, Reischbach G, Feederle R, et al. The EBV nuclear antigen 1 (EBNA1) enhances B cell immortalization several thousand fold. *Proc Natl Acad Sci U S A*. 2003;100:10989-94.

Y Li 李 艷  
L Fu 付 利  
AM Wong  
YH Fan 范彦輝  
MX Li 李淼新  
JX Bei  
WH Jia 賈衛華  
YX Zeng 曾益新  
D Chan 陳振勝  
KM Cheung 張文智  
P Sham 沈伯松  
D Chua 蔡清澳  
XY Guan 關新元  
YQ Song 宋又強

# Fine mapping candidate loci for nasopharyngeal carcinoma in southern Chinese specifically linked to Epstein-Barr virus aetiopathogenesis

## Key Messages

1. Nasopharyngeal carcinoma (NPC) is a malignancy of epithelial origin.
2. The aetiology of NPC is complex and includes multiple genetic and environmental factors.
3. Genetic factors for NPC were detected on chromosome 6p regions.

## Introduction

Nasopharyngeal carcinoma (NPC) is of epithelial origin. Its aetiology is complex and comprises multiple genetic and environmental factors. There are distinct geographical and ethnic differences in its incidence. In Southeast Asians, particularly from the Chinese province of Guangdong, susceptibility to NPC is nearly 100-fold higher than in most persons from European countries. Thus, NPC is regarded as the 'Cantonese' cancer, with incidences ranging from 10 to 50 cases per 100 000 inhabitants in this region.<sup>1</sup> This NPC epidemic also shows familial aggregation.

Genetic linkage studies and the candidate-gene-based approach have been used to identify NPC susceptibility genes.<sup>2</sup> Notably, chromosome 6 super loci containing the human leukocyte antigen (HLA) system has been linked to the pathogenesis of NPC.<sup>3-5</sup> Two genome-wide association studies (GWAS) to scan the whole human genome for disease susceptibility loci reported an increased susceptibility in southern Chinese.<sup>3,5</sup>

The linkage of NPC to 6p21.3 provides a genetic basis for a more thorough linkage analysis for disease susceptible loci in different populations. We studied the NPC-associated genetic markers using case-control analysis. The top 15 NPC genes within the linkage region were chosen from PubMed references, and then tag single nucleotide polymorphisms (tag SNPs) within the genes were selected from the HapMap CHB database. In total, 233 tag SNPs on chromosome 6p were selected to test whether they were associated with NPC in the southern Chinese.

## Methods

This study was conducted from January 2009 to December 2010. Ethics approval for this study and written informed consent from all participants were obtained. The disease group included 360 patients of southern Chinese descent from Guangdong with pathologically confirmed diagnosis of NPC. Their mean±standard deviation (SD) age was 46.4±11.2 years; 72% were males. The control group included 360 southern Chinese subjects with degenerate disc disease. Their mean±SD age was 41.4±8.9 years; 66% were females.

The SNPs were selected based on the candidate gene. According to the degenerate disc disease study, the whole genome scan data had 17 313 SNPs genotyped on chromosome 6. Focusing solely on the genes located in the candidate region identified by the meta-analysis of the top candidate genes, 2730 SNPs remained. Only 233 tag SNPs were selected for genotyping.

The MassARRAY Assay genotyping method (Sequenom) was used to genotype according to the manufacturer's protocol. The genotyping of 12 significant SNPs from a Taiwanese group was conducted using ABI Taqman SNP genotyping assays. Human pre-designed Taqman probes were provided by

*Hong Kong Med J* 2013;19(Suppl 5):S43-6

The University of Hong Kong:  
Department of Biochemistry  
Y Li, YH Fan, MX Li, D Chan, YQ Song  
Department of Clinical Oncology  
L Fu, AM Wong, D Chua, XY Guan  
Department of Orthopaedics and  
Traumatology  
KM Cheung  
Department of Psychiatry  
P Sham  
State Key Lab of Oncology in Southern  
China & Department of Experimental  
Research, Sun Yat-sen University Cancer  
Centre, Guangzhou, China  
JX Bei, WH Jia, YX Zeng

RFICID project number: 08070652

Principal applicant and corresponding author:  
Dr Song You-Qiang  
L3-63, Lab Block, 21 Sassoon Road,  
Pokfulam, Hong Kong SAR, China  
Tel: (852) 2819 9245  
Fax: (852) 2855 1254  
Email: songy@hku.hk

the Taiwanese group. Real-time data were analysed using the SDS 2.3 application provided by ABI.

To examine candidate gene expression, 20 primary NPC biopsies and adjacent normal tissues at the resection margins were collected immediately after surgical resection at Queen Mary Hospital in Hong Kong. The three NPC cell lines used (CNE2, SUNE1, and C666-1) were maintained in RPMI-1640 medium and supplemented with 10% foetal bovine serum. An immortalised nasopharyngeal epithelial cell line (NP69) was also cultured.

Total RNA from the cell lines was extracted using the Trizol reagent and following the manufacturer's protocol. The Transcriptor High Fidelity cDNA Synthesis Kit was used to synthesise cDNA.

For quantitative PCR analysis, cDNA was subjected to amplification with the SYBR Green PCR Kit using primers for NEDD9 and GABBR1. Human 18S rRNA was used as the endogenous control. The threshold cycle was determined in real time using an ABI PRISM 7700 Sequence Detector.

The association analyses were performed by the PLINK and Haploview 4.2 method. The haplotype structure was also analysed by PLINK using the three-SNP sliding window option. Multiple testing was performed with 10 000 permutations and/or with Bonferroni correction. LocusZoom was used to generate the association plot.

## Results

### *Genetic association study of 6p SNPs in southern Chinese*

The overall genotyping call rate was  $\geq 97.8\%$ . Genotyped SNPs were arranged according to their physical locations on chromosome 6 and allelic associations ( $-\log^{10} P$  values). The most significant association was found for SNP rs2076483 ( $P=3.36 \times 10^{-5}$ ). Two adjacent SNPs, rs2267633 ( $P=4.49 \times 10^{-5}$ ) and rs29230 ( $P=1.43 \times 10^{-4}$ ), located at the 6p23.31 region also showed high significance, suggesting that this region was significantly associated with NPC (data not shown).

### *Haplotype analysis of the GABBR1 and HLA-A gene regions*

The most significantly associated haplotypes—AAA ( $P=6.46 \times 10^{-5}$ ) and GGG ( $P=1.0 \times 10^{-4}$ )—were located within GABBR1 and comprised three significant SNPs (rs2267633, rs2076483, and rs29230). Haplotype AAA of GABBR1 had a highly significant  $P$  value of  $6.46 \times 10^{-5}$ . This indicates that individuals carrying the AAA haplotype could be more susceptible to NPC than GGG carriers. In contrast, the haplotype GG composed of rs2517713 and rs2975042 within the HLA-A gene showed a protective effect against NPC ( $P=7.0 \times 10^{-4}$ ), whereas the haplotype TT exhibited high risk of NPC disease (TT,  $P=0.0014$ ).

Multiple testing correction was conducted with 10 000 permutations; haplotypes AAA ( $P=0.0008$ ) and GGG ( $P=0.0010$ ) of GABBR1 and haplotypes GG ( $P=0.0072$ ) and TT ( $P=0.0134$ ) of HLA-A all survived the multiple testing.

Using the three-SNP sliding windows, haplotypes AAA and GGG formed by significant SNPs (rs2267633, rs2076483, and rs29230) reached statistical significance ( $P=7.610 \times 10^{-5}$  and  $P=7.614 \times 10^{-5}$ , respectively). Two SNPs haplotypes formed by rs2517713 and rs2975042 were GG and TT, with  $P$  values of 0.00078 and 0.00078, respectively, and were even more significant than Haploview results.

### *Loss of heterozygosity and micro-deletions at 6p as detected by SNP genotyping*

The high resolution of the SNP array and the large sample size enabled us to monitor the small DNA copy number changes occurring in NPC. To identify the micro-deletions at 6p in NPC, the frequency of the homozygous genotype in controls and cases should be determined first. For each SNP marker, the ratio of homozygous frequency between the cases and the controls (T/N ratio) was calculated. Using a threshold T/N ratio of  $>1.0$ , 19 loci that reached statistical significance were considered loci liable to frequent loss of heterozygosity (LOH). The micro-deleted region was defined when three or more adjacent SNP markers were considered frequent LOH loci. Three micro-deletions were identified at 6p25-24, 6p21.31, and 6p21.3 (Table). The small deletions on 6p affected several genes, including glucosaminyl (N-acetyl) transferase 2, I-branching enzyme (GCNT2), (NEDD9), and GABBR1 (Table). The genes at 6p21.3 were pseudogenes and thus not further studied. The GCNT2 gene has never been linked to cancer development. NEDD9 and GABBR1 were the most promising potential candidate genes. We examined their mRNA expression levels in different cell lines and tissues.

### *Examination of mRNA expression of candidate NPC susceptibility genes*

To study the two candidate genes for the development of NPC, mRNA expression was characterised by quantitative real-time PCR in three NPC cell lines (CNE2, SUNE1, and C666-1) in the immortalised normal nasopharyngeal epithelial cell line NP69, and in 11 primary NPC tissue samples with adjacent normal tissue. Compared to the normal nasopharyngeal epithelial cell line NP69, the SUNE1 and C666-1 cells demonstrated lower NEDD9 mRNA expression. Conversely, the CNE2 cell line displayed an estimated 4-fold increase in NEDD9 expression (data not shown). Compared with adjacent non-tumour tissue, 10 of 11 NPC tumour biopsy samples showed a significant downregulation of NEDD9 ( $P=0.015$ ; data not shown). Moreover, GABBR1 was downregulated in all three NPC cell lines (data not shown) and in eight of 11 tumour biopsy tissues (data not shown). The GABBR1 gene showed a marginally significant association between the NPC tumour and non-tumour tissue specimens ( $P=0.059$ ).

**Table. Summary of frequent loss of heterozygosity loci at 6p detected by single nucleotide polymorphism (SNP) array**

SNP ID*	Location	Homozygous frequency ratio of cases/controls	P value	Gene
rs2085575	6p25.3-24.3	1.2073538	0.004	F13A1
rs3024317	6p25.3-24.3	1.1449631	0.0181	F13A1
rs4960294	6p25	1.1457735	0.0298	RREB1
rs6597256	6p25	1.1318706	0.017	RREB1
rs267184	6p24-23	1.1431448	0.0253	BMP6
rs504083	6p24.2	1.1581754	0.0281	GCNT2
rs1318748	6p24.2	1.1529571	0.0371	GCNT2
rs11759513	6p25-24	1.1893557	0.0232	NEDD9
rs2137873	6p23	1.1861716	0.011	ATXN1
rs235147	6p23	1.1638418	0.03	ATXN1
rs236949	6p23	1.1905564	0.0047	ATXN1
rs2143083	6p22.3-22.2	1.3092179	0.0001	ALDH5A1
rs2267633	6p21.31	1.1809524	0.0033	GABBR1
rs2076483	6p21.31	1.2159952	0.0007	GABBR1
rs29230	6p21.31	1.1642882	0.0007	GABBR1
rs2517713	6p21.3	1.1925186	0.0109	HCP5P3
rs9260734	6p21.3	1.2099734	0.0033	HCG2P6
rs3869062	6p21.3	1.1733857	0.0101	HCG2P6
rs5009448	6p21.3	1.1841842	0.0164	MICD

\* SNP markers at micro-deleted region in bold

## Discussion

Multiple loci within 6p21.3 were associated with NPC susceptibility. Using samples from southern China, we found significant allelic and haplotype associations with NPC. Consistent with other reports,<sup>3-5</sup> the HLA-A region was significantly associated with NPC. The most significant SNPs were similar to those found in a Taiwanese GWAS.<sup>3</sup> The subjects analysed were all southern Chinese and the MAFs were similar; such deviation might be due to genetic heterogeneity.

### *GABBR1 underscores a possible role in the aetiology of NPC*

Two candidate genes located within the micro-deleted regions, NEDD9 at 6p25-24 and GABBR1 at 6p21.31, were absent or downregulated at the mRNA expression level in primary NPC tumours and NPC cell lines. Although the sample size (n=11) used for quantitative real-time PCR analysis was not sufficient for statistical calculation, the quantitative PCR results did show alterations in gene expression levels. The different expression changes were from the copy number variations in the tumour DNA, and no direct link to the micro-deletion was detected when comparing the normal DNA in cases and controls. However, the different expression levels of NEDD9 and GABBR1 between PNC tumours and normal tissues indicated the importance of both genes in NPC development. A population-based study to determine whether micro-deletion in normal DNAs can also reduce GABBR1 expression is warranted. This study provides the first evidence that the NEDD9 gene is subject to down-regulation at the transcriptional level due to copy number loss in NPC tumours.

The Taiwan GWAS was the first study to associate GABBR1 with NPC and reported elevated GABBR1 protein expression in NPC tumour tissues (compared with

the adjacent normal epithelial cells).<sup>3</sup> In another GWAS conducted in Guangzhou,<sup>5</sup> the strong association within the HLA regions on 6p was validated. In addition, three new NPC susceptibility loci were detected on 3q26, 9p21, and 13q12, and novel risk genes were also identified. Other candidate genes and cancer genesis mechanisms could underlie the NPC pathogenic process. In view of the high prevalence of NPC in the southern Chinese population, future studies on NPC should focus on novel pathogenic loci to discover new tumourigenic genes and provide clinical targets for treatment.

## Conclusions

Significant single-marker associations were found for SNPs rs2267633 ( $P=4.49 \times 10^{-5}$ ), rs2076483 ( $P=3.36 \times 10^{-5}$ ), and rs29230 ( $P=1.43 \times 10^{-4}$ ). Multiple chromosome 6p susceptibility loci contributed to the risk of NPC.

## Acknowledgements

This study was supported by the Research Fund for the Control of Infectious Diseases, Food and Health Bureau, Hong Kong SAR Government (#08070652). Genotype information for controls was from a project supported by AO Foundation (AOSBRC-07-02).

## References

1. Ho JH. An epidemiologic and clinical study of nasopharyngeal carcinoma. *Int J Radiat Oncol Biol Phys* 1978;4:182-98.
2. Zhou X, Cui J, Macias V, et al. The progress on genetic analysis of nasopharyngeal carcinoma. *Comp Funct Genomics* 2007;57513.
3. Tse KP, Su WH, Chang KP, et al. Genome-wide association study reveals multiple nasopharyngeal carcinoma-associated loci within the HLA region at chromosome 6p21.3. *Am J Hum Genet* 2009;85:194-203.
4. Lu SJ, Day NE, Degos L, et al. Linkage of a nasopharyngeal carcinoma

- susceptibility locus to the HLA region. *Nature* 1990;346:470-1.
5. Bei JX, Li Y, Jia WH, et al. A genome-wide association study of nasopharyngeal carcinoma identifies three new susceptibility loci. *Nat Genet* 2010;42:599-603.

## AUTHOR INDEX

---

Au MTK	4	Leung ETY	8
Au SW	27	Leung KK	12
Bei JX	43	Leung KS	12
Chan AWH	36	Leung PPS	36
Chan D	43	Li CH	24
Chan EWC	4, 8	Li JCB	15, 19
Chan LLY	19	Li MX	43
Chan RCY	4, 8, 12	Li Y	43
Chau SL	31, 36	Ling WL	15
Chen Y	24	Lo KW	31, 36
Cheung BKW	19	Lou SK	12
Cheung KM	43	Lung RWM	31, 36
Cho CH	27	Ng DCH	36
Chua D	43	Ng EKO	36
Fan YH	43	Ng TB	27
Fang JW	15	Rolka K	27
Fu L	43	Sham P	43
Fung KP	12	Song YQ	43
Gu OW	27	Sung MYM	31, 36
Guan XY	43	To KF	31, 36
Hui M	27	Tong JHM	31, 36
Ip M	8	Tsui SKW	12
Jia WH	43	Wan DC	27
Jin HC	39	Wang VLJ	15
Kam KM	12	Waye MMY	12
Kwan HS	12	Wong AM	43
Lai RWM	4	Wong BC	24
Lam WW	27	Wong JH	27
Lau ASY	15, 19	Yim HCH	19
Law PTW	12	Yu J	39
Lee DCW	19	Zeng YX	43
Lee SS	24	Zhang X	24
Legowska A	27		

### **Disclaimer**

The reports contained in this publication are for reference only and should not be regarded as a substitute for professional advice. The Government shall not be liable for any loss or damage, howsoever caused, arising from any information contained in these reports. The Government shall not be liable for any inaccuracies, incompleteness, omissions, mistakes or errors in these reports, or for any loss or damage arising from information presented herein. The opinions, findings, conclusions and recommendations expressed in this report are those of the authors of these reports, and do not necessarily reflect the views of the Government. Nothing herein shall affect the copyright and other intellectual property rights in the information and material contained in these reports. All intellectual property rights and any other rights, if any, in relation to the contents of these reports are hereby reserved. The material herein may be reproduced for personal use but may not be reproduced or distributed for commercial purposes or any other exploitation without the prior written consent of the Government. Nothing contained in these reports shall constitute any of the authors of these reports an employer, employee, servant, agent or partner of the Government.

Published by the Hong Kong Academy of Medicine Press for the Government of the Hong Kong Special Administrative Region. The opinions expressed in the *Hong Kong Medical Journal* and its supplements are those of the authors and do not reflect the official policies of the Hong Kong Academy of Medicine, the Hong Kong Medical Association, the institutions to which the authors are affiliated, or those of the publisher.